

# Population dynamics of *Varroa* mite and honeybee: Effects of parasitism with age structure and seasonality

Komi Messan<sup>a</sup>, Marisabel Rodriguez Messan<sup>b</sup>, Jun Chen<sup>a</sup>, Gloria DeGrandi-Hoffman<sup>c</sup>, Yun Kang<sup>d</sup>

<sup>a</sup>*Simon A. Levin Mathematical and Computational Modeling Sciences Center, Arizona State University, Tempe, AZ 85281, USA.*

<sup>b</sup>*Department of Ecology and Evolutionary Biology, Brown University, Providence RI 02912 USA*

<sup>c</sup>*Carl Hayden Bee Research Center, United States Department of Agriculture-Agricultural Research Service, Tucson, AZ 85719, USA.*

<sup>d</sup>*Sciences and Mathematics Faculty, College of Integrative Sciences and Arts, Arizona State University, Mesa, AZ 85212, USA.*

---

## Abstract

Honeybees play an important role in sustaining the ecosystem. However, the rapid decline of honeybee population have sparked a great concern worldwide. Field and theoretical studies have shown that the infestation of the parasitic *Varroa* mite (*Varroa destructor* Anderson and Trueman) could be one of the main reasons that lead to colony collapsing. In order to understand how mites affect population dynamics of honeybees and the healthy status of colony, we propose and study a brood-adultbee-mite interaction model in which the time lag from brood to adult bee is taken into account. Noting that the temporal dynamics of honeybee colony varies with respect to changes in seasonality, we validate the model and perform parameter estimations under both constant and fluctuating seasonality scenarios. Our analytical and numerical studies reveal the following: (a) In the presence of parasite mites, the large time lag from brood to adult bee could destabilize population dynamics and drive the colony to collapse; however the small natural mortality of adult bee population has the ability to promote a mite-free colony when time lag is small or at an intermediate level; (b) Small brood's infestation rate could stabilize all populations at the unique interior equilibrium under constant seasonality while driving the mite population to die out when changes in seasonality is taken into account; (c) Large brood's infestation rate can destabilize the dynamics leading to colony collapse depending on initial population size under constant and non-constant seasonal model; (d) Results from our sensitivity analysis indicate that the queen's egg-laying may have the greatest effect on colony population size. The death rate of the brood and the colony size at which brood survivability is half maximal were also shown to be highly sensitive with an inverse correlation to the colony population size. Our results provide great insights on the dynamics generated by seasonality where the mite population dies out leaving healthy colony with brood and adult bee in the presence of seasonality while all population goes extinct without seasonality.

**Keywords:** Honeybee, *Varroa* mite, Colony loss, Seasonality, Delay Differential Equations

---

*Email addresses:* Komi.S.Messan@erd.c.dren.mil (Komi Messan), Marisabel@asu.edu (Marisabel Rodriguez Messan), jchen152@asu.edu (Jun Chen), gloria.hoffman@ars.usda.gov (Gloria DeGrandi-Hoffman), yun.kang@asu.edu (Yun Kang)

---

## 1. Introduction

Honeybees (*Apis mellifera*) are exemplars of social evolution, known for their complex social organization [41], and are the most economically valuable pollinators of crops in the world [19, 36]. However, honeybees have posed an increase of colony mortality, including colony collapsing disorder (CCD), and overwinter or seasonal colony losses [19, 47, 62]. The dynamics within a honeybee colony is a complex phenomenon characterized by different behaviors. Such behaviors include reproductive and worker division of labor which allow the performance of ‘basic’ but important activities like the reproduction of the queen bee and tasks done by workers (e.g brood rearing and foraging). Specifically, brood rearing and colony growth depend on queen’s egg-laying activity which in return rely upon successful foraging activity by the workers making the dynamics a feedback system of interdependent elements [15].

Honeybees must go through an optimal collective-decision making process in order to sustain the colony. Several field and laboratory experiments including [24, 63, 64] have shown how bees are able to select the most profitable food source in an explored environment. [24] also found a direct relationship between pollen storage levels and colony brood production, demonstrating the potential for cumulative changes in individual foraging decisions that affect colony fitness. As a part of this decision making, honeybees must also defend their colonies against many hazards including robber bees, diseases, and parasitism. For instance, [22] describes some of the behavioral mechanisms bees use for reducing the disease risk of their nest. Moreover, hygienic behavior and grooming have been shown to be the two main mechanisms bees are prone to use as defense against diseases and parasitisms [5]. Unfortunately, honeybees are increasingly threatened and challenged by different factors including diseases (e.g American and European foulbrood, Chalkbrood, Stonebrood, Nosema, etc.), parasitism (e.g. mites), and nutritional stress [48]. Most notably, the *Varroa* mite has posed a huge threat on the honeybees well-being [12, 13, 27, 29, 35, 37, 60, 61].

The *Varroa* mite is the most adverse parasite of the honeybee associated with a high percentage of colony losses over the winter [37]. Mites affect honeybees in different aspects either by direct physical damage or activation of viruses [37]. For instance, parasitized bee brood develop into adults with shorter abdomens, deformed wings (virus related) and shorter lifespans [2, 10, 37] through the suppressed expression of genes related to longevity and development (e.g. storage protein, vitellogenin, etc.) [46]. Also, foragers parasitized by *Varroa* are more likely to get lost and wander between colonies [37, 38]. It is noteworthy to point out that *Varroa* mites only reproduce in both capped worker and drone brood cells, thus making brood’s availability in colonies paramount for mites reproduction [12]. Mites can however parasitize both bee brood and adult bees, and are rarely found on queens [12].

The spread of mites through the bee population can be both vertically, i.e., phoretic mites travel upon the swarming bees, and horizontally, i.e., wandering and robbing honey from other colonies and movement of infested brood or bees by beekeepers [51]. The reproduction of *Varroa* occurs in capped worker and drone brood cells when a mature female mite (foundress) enters the cell preceding capping [12, 54]. The foundress starts feeding on the brood and continues to feed regularly

thereafter [18]. The foundress lays its first egg which develops into a male and the second one into a female mite that mates with the male [12]. The mother mite keeps feeding on the developing larva, which in the process, transmits several different viruses [12]. After the bee is fully developed and emerges from the capped cell, the mother mite and offsprings emerge with it and attach to other adult bees as “phoretic mites” [12]. In general, phoretic mites target nurse bees [9, 17] because they remain in the brood area and serve as a medium to transport mites to brood cells where they can reproduce [12]. In recent years, the reproductive rates of *Varroa* have exceeded those expected [11–13], therefore becoming a major factor in colony losses.

Mathematical models have been powerful tools to help us understand the effects of mites (e.g., [35]), disease (e.g. [35, 52]), and pesticides (e.g., [49, 50]) on honeybee population dynamics. There are some models that are introduced to explore the role of mite infestation in honeybee colonies (see the work of [39, 45, 52, 53]). [35] proposed a honeybee-mite-virus model that incorporates parasitic interactions between honeybees and the *Varroa* mites in addition to a virus transmission dynamics. It was found that low adult bee to brood ratios have destabilizing effects on the system, generate fluctuating dynamics, and potentially lead to a catastrophic event where both honeybees and mites suddenly become extinct within a colony. However, [35] did not explicitly modeled the brood population thus omitting the role of brood population size on mite’s proliferation. [3] constructed an agent-based model to explore how various stressors (including *Varroa* mites, virus infections, impaired foraging behavior, changes in landscape structure, pesticides, etc.) affect the performance of single managed colonies of honeybees. While the latter work provides valuable results on different mechanisms that may induce the decline of honeybee population in a colony, brood population was not taken into account explicitly. An another approach on studying the effects of *Varroa* mites infestation on honeybees through dispersal mechanism was done on [45]. This study contains a complete analysis of local and global dynamics of a two-patch model that incorporates mite migration through foraging activities of bees. The results of this study provide insight on different scenarios where different migration rates can affect the bee population negatively or drive the mite population extinct within the colony. However, this study lacks focus on the different population dynamics that can arise within a colony from mechanism such as reproduction and parasitism of mites on brood and adult bees.

The first honeybee modeling paper by DeGrandi-Hoffman (see [15]) proposed a simulated model which illustrates the role of certain life history parameters in the honeybee colony population dynamics by incorporating colony population size (i.e. proportion of workers and drones), weather conditions, forager longevity, and the queen’s reproductive state. Motivated by the work of [15, 45], we introduce a single patch stage structure delay differential equation model that considers the time lag from brood to adult bee. The modeling framework used here is inspired by the work of [1]. By including the mite parasitism effects and reproductive mechanisms to the life cycle of the bees, the model proposed here is used to assess the effects of different parameters affecting the population size of a colony. More specifically, we aim to use this model to explore how the synergistic effects of age structure and parasitism affect the colony dynamics in seasonal environment.

In the following two sections (2&3), we provide a detailed derivation of the proposed model, and perform mathematical analysis and the related theoretical results with their consequent biological interpretations. In section 4, we provide a description of the data used for model validation,

parameter estimation and sensitivity analysis. The dynamical outcomes of mite infestation within a colony is also presented in section 5. In section 6, we discuss the findings, related biological interpretations and final thoughts. The detailed proofs of theoretical results, tables, and additional diagrams are collected in the appendix.

## 2. Model Derivation

Let  $B(t)$ ,  $H(t)$ , and  $M(t)$  denote the total population of brood, adult honeybee, and mites at time  $t$ , respectively. Following the schematic diagram in Figure (1), our model has the following assumptions:

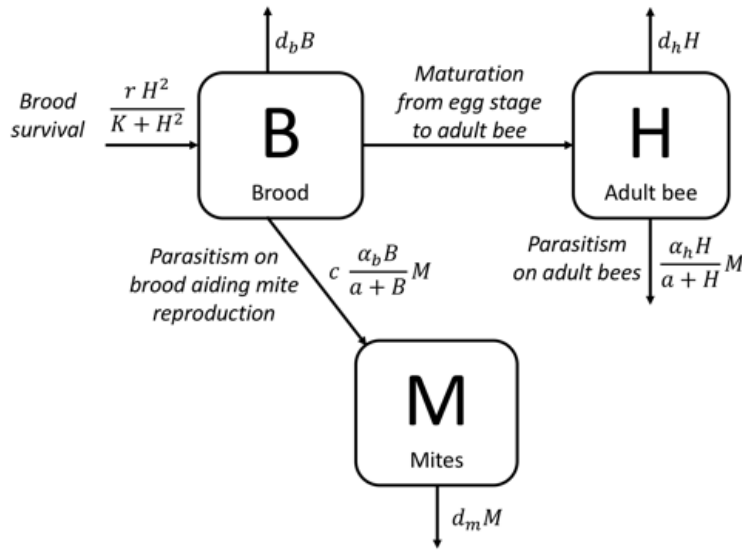


Figure 1: Schematic diagram for the honeybee-mite parasitic interaction.

Let  $\tau > 0$  be the time interval in which the population entering an homogeneous environment equal to the length of time from egg to fully developed adult bee. We assume that the interval where both populations are known is  $-\tau \leq t \leq 0$ . Let  $B_0(t)$  be the observed or assumed egg-laying rate of  $B(t)$  at time  $t$ ,  $-\tau \leq t \leq 0$ . Let  $H(0)$  and  $M(0)$  be the observed value of  $H(t)$  and  $M(t)$ , respectively, at time  $t = 0$ . Our model is derived as follows and takes one form on the interval  $0 < t \leq \tau$  and second form on the interval  $t > \tau$ :

1. We assume that at any time  $t > 0$  the brood population,  $B$ , increases through the successful survivability of an egg into pupae stage represented by the term  $\frac{H^2}{K+H^2}$ , which incorporates the collaborative efforts of adult workers, via division of labor. This term assumes that successful colonies produce more brood and efficient workers, an assumption supported by the literature work [21, 35, 57].

2. The brood, adult bee, and mite populations are assumed to have a natural average death rate proportional to that existing population denoted with constant parameters  $d_b$ ,  $d_h$ , and  $d_m$ , respectively.
3. The brood and adult bee population decreases through the parasitism effect of mites. The probability of mites attaching to brood and adult bees is modeled with the terms  $\frac{B}{a+B}$  and  $\frac{H}{a+H}$ , respectively, where  $a$  is the size of the brood or adult bee population, accordingly, at which the rate of attachment is half maximal (see a similar approach in [4, 60]). The parameters  $\alpha_b$  and  $\alpha_h$  measure the parasitism rate of mites on the brood and adult bees, respectively.
4. The mite population increases through the parasitism effects of brood which aids mite reproduction. The work of [6, 26, 59] suggests that initiation of oocyte development in *Varroa jacobsoni* depends on whether the female enters the brood cell of *Apis mellifera* before operculation, thus, the term  $\frac{c\alpha_b B}{a+B}$  accounts for the production of new mites, where  $c$  is the conversion factor from brood to mite population. The mite model could hence be described by:

$$\frac{dM}{dt} = \left[ \frac{c\alpha_b B}{a+B} - d_m \right] M \quad (1)$$

5. The life cycle of the female *Varroa* mite is normally subdivided into a phoretic phase in which it lives on adult bees and a reproductive phase occurring within worker or drone brood cells, thus, the two life stages should be modeled explicitly. However, from the work of [35, 45], we assume an implicit age structure for the mite population where the ratio of different stages are constant. For example, consider  $\xi \in [0, 1]$  the percentage of mites at the non-phoretic stage, then  $(1 - \xi)M$  is the phoretic mite population. Let  $\hat{d}_m = d_m(1 - \xi)$  and the phoretic mite becomes

$$\frac{dM}{dt} = \frac{c\alpha_b BM}{a+B} - d_m(1 - \xi)M = \frac{c\alpha_b BM}{a+B} - \hat{d}_m M.$$

Similar approach can be follow to find the reproductive mite population and by grouping the reproductive and phoretic mites together, we obtain the mite model defined in (1).

6. We assume that eggs laid at time  $t - \tau$  that survive to time  $t$ , i.e.  $\frac{rH(t-\tau)^2}{K+H(t-\tau)^2}$ , exit (or mature) from the brood population  $B$  and enter the adult bee population  $H$ . The survival of the brood population depends on their own natural death and if they outlive the mite infestation. Therefore, the probability of survival is  $e^{-\int_{t-\tau}^t (d_b + \frac{\alpha_b M(s)}{a+B(s)}) ds}$  when  $0 < t \leq \tau$  and  $t > \tau$ . We follow a similar approach and derivation in [1] and obtain the number of brood that survive into adult bee:

$$B_0(t - \tau) e^{-\int_{t-\tau}^t (d_b + \frac{\alpha_b M(s)}{a+B(s)}) ds} \quad \text{when} \quad 0 < t \leq \tau$$

and

$$\frac{rH(t - \tau)^2}{K + H(t - \tau)^2} e^{-\int_{t-\tau}^t (d_b + \frac{\alpha_b M(s)}{a+B(s)}) ds} \quad \text{when} \quad t > \tau.$$

7. For continuity of initial conditions, ecological reasons, and following similar approach in [1], the total surviving brood population from the observed eggs laid on  $-\tau \leq t \leq 0$  is

$$B(0) = \int_{-\tau}^0 B_0(t) \exp \left\{ - \int_t^0 \left( d_b + \alpha_b \frac{M_0(s)}{a + B_0(s)} \right) ds \right\} dt = \int_{-\tau}^0 B_0(t) dt > 0.$$

The model formulated by the assumptions provided above is therefore composed by two time intervals,  $0 < t \leq \tau$  and  $t > \tau$ , in the following form:

• **Model for  $t \in (0, \tau]$**

$$\begin{aligned}
\frac{dB}{dt} &= \underbrace{\frac{rH^2}{K+H^2}}_{\text{egg production}} - \underbrace{\alpha_b \frac{\overbrace{B}^{\text{probability of } M \text{ attaching to } B}}{a+B} M}_{\text{parasitism on brood}} - \underbrace{d_b B}_{\text{natural death}} - \underbrace{e^{-\int_{t-\tau}^t [d_b + \frac{\alpha_b M(s)}{a+B(s)}] ds} B_0(t-\tau)}_{\text{maturation from egg to adult}} \\
\frac{dH}{dt} &= \underbrace{e^{-\int_{t-\tau}^t [d_b + \frac{\alpha_b M(s)}{a+B(s)}] ds} B_0(t-\tau)}_{\text{transition from brood}} - \underbrace{\alpha_h \frac{\overbrace{H}^{\text{probability of } M \text{ attaching to } H}}{a+H} M}_{\text{parasitism on adult bee}} - \underbrace{d_h H}_{\text{natural death}} \\
\frac{dM}{dt} &= \underbrace{c\alpha_b \frac{B}{a+B} M}_{\text{newborns from brood parasitism}} - \underbrace{d_m M}_{\text{natural death}}
\end{aligned} \tag{2}$$

• **Model for  $t > \tau$**

$$\begin{aligned}
\frac{dB}{dt} &= \underbrace{\frac{rH^2}{K+H^2}}_{\text{egg production}} - \underbrace{\alpha_b \frac{\overbrace{B}^{\text{probability of } M \text{ attaching to } B}}{a+B} M}_{\text{parasitism on brood}} - \underbrace{d_b B}_{\text{natural death}} - \underbrace{\frac{e^{-\int_{t-\tau}^t [d_b + \frac{\alpha_b M(s)}{a+B(s)}] ds} rH(t-\tau)^2}{K+H(t-\tau)^2}}_{\text{maturation from egg to adult}} \\
\frac{dH}{dt} &= \underbrace{\frac{e^{-\int_{t-\tau}^t [d_b + \frac{\alpha_b M(s)}{a+B(s)}] ds} rH(t-\tau)^2}{K+H(t-\tau)^2}}_{\text{transition from brood}} - \underbrace{\alpha_h \frac{\overbrace{H}^{\text{probability of } M \text{ attaching to } H}}{a+H} M}_{\text{parasitism on adult bee}} - \underbrace{d_h H}_{\text{natural death}} \\
\frac{dM}{dt} &= \underbrace{c\alpha_b \frac{B}{a+B} M}_{\text{newborns from brood parasitism}} - \underbrace{d_m M}_{\text{natural death}}
\end{aligned} \tag{3}$$

with initial conditions

$$B(t) = B_0(t) > 0, M(t) = M_0(t) > 0, t \in [-\tau, 0], H(0) > 0, \tag{4}$$

where  $B_0(t), M_0(t) \in \mathcal{C} := C([-\tau, 0], [0, +\infty))$  are the population of eggs and adults, respectively, at  $t \in [-\tau, 0]$ .

In the next section, we will compare dynamics of our proposed model with/without parasite  $M(t)$  to gain insights on the effects of mites.

Parameter	Description	Estimate/Units	Reference
$r$	maximum egg-laying rate by the queen	0, 500, 1500 bees/day (season dependent)	[20, 60]
$d_b$	average death rate of brood (larvae and pupae stage)	† 0.00602-0.036 (unsealed brood); 0.00303 (sealed brood) day <sup>-1</sup>	[25]
$d_h$	average death rate of adult honeybee	0-0.17 (hive bees); 0-0.8 (foragers) day <sup>-1</sup>	[55]
$d_m$	average death rate of phoretic mite	(0.016-0.45) or 0.002 (winter), 0.006 (summer) day <sup>-1</sup>	[7, 43]
$c$	conversion rate from mite feeding on honeybee to mite reproduction	0-4.5	[31]
$\sqrt{K}$	colony size at which brood survivability is half maximal	≤ 22007 (fall, spring), and ≤ 37500 (summer) bees/day (upper bound values)	[52]
$\alpha_b$	parasitism rate on brood	0.0447 day <sup>-1</sup>	Estimated from data
$\alpha_h$	parasitism rate on adult bee	0.8 day <sup>-1</sup>	Estimated from data
$a$	size of honeybee population at which rate of attachment is half maximal	8050 bees	Estimated from data
$\tau$	Brood development time from egg to adult bee	16 (queens), 21 (workers), 24 (drones) days	P. 83 in [28]

Table 1: Standard parameters values used for simulation of honeybee and mite population of Model (2)-(3). † calculated from the daily mortality ( $[1 - \frac{330}{332}]$ ,  $[1 - \frac{347}{360}]$ ) for unsealed brood and  $(1 - \frac{329}{330})$  for sealed brood.

### 3. Mathematical Analysis

We first provide the basic dynamical properties of Model (2)-(3) as follows:

**Theorem 3.1.** *Solution  $(B(t), H(t), M(t))$  of System (2)-(3) satisfying (4) is positive for all  $t > 0$ . In addition,*

$$\limsup_{t \rightarrow \infty} (B(t) + H(t) + M(t)) \leq \frac{cr}{\min\{d_b, d_h, d_m\}}.$$

**Biological Implications:** Theorem 3.1 implies that Model (2)-(3) is well-defined biologically as it is positively invariant and bounded.

#### 3.1. Dynamics of Honeybee

The honeybee-mite system (2)-(3) reduces to the following honeybee-only subsystem (5)-(6) when  $M(0) = 0$ :

- Model for  $t \in (0, \tau]$

$$\begin{aligned}\frac{dB}{dt} &= \frac{rH^2(t)}{K + H^2(t)} - d_b B(t) - e^{-d_b \tau} B_0(t - \tau) \\ \frac{dH}{dt} &= e^{-d_b \tau} B_0(t - \tau) - d_h H(t)\end{aligned}\tag{5}$$

- Model for  $t > \tau$

$$\begin{aligned}\frac{dB}{dt} &= \frac{rH^2(t)}{K + H^2(t)} - d_b B(t) - e^{-d_b \tau} \frac{rH^2(t - \tau)}{K + H^2(t - \tau)} \\ \frac{dH}{dt} &= e^{-d_b \tau} \frac{rH^2(t - \tau)}{K + H^2(t - \tau)} - d_h H(t)\end{aligned}\tag{6}$$

The detailed dynamics of the honeybee-only subsystem (5)-(6) have been studied in [34]. Note that its extinction equilibrium  $E_e = (0, 0)$  is always an equilibrium. Let

$$H_{1,2}^* = \frac{r e^{-d_b \tau}}{2d_h} \left( 1 \pm \sqrt{1 - \left( \frac{2d_h e^{d_b \tau}}{r} \right)^2 K} \right),\tag{7}$$

with  $H_1^* \leq H_2^*$ , hence the subsystem (5)-(6) has two interior equilibria  $E_i = (B_i^*, H_i^*)$  with

$$B_i^* = \frac{1}{d_b} (1 - e^{-d_b \tau}) \frac{r(H_i^*)^2}{K + (H_i^*)^2} = \frac{d_h (e^{d_b \tau} - 1)}{d_b} H_i^*, i = 1, 2.\tag{8}$$

Based on the work of Jun (cite here), we summarize dynamical results of the subsystem (5)-(6) as follows (also see Table 2):

1. The extinction equilibrium  $E_e$  of the subsystem (5)-(6) always exists and is always locally asymptotically stable.
2. If  $\frac{r}{d_h} < 2e^{d_b \tau} \sqrt{K}$ , the subsystem (5)-(6) has its global stability at the extinction equilibrium  $E_e$ .
3. If  $\frac{r}{d_h} = 2e^{d_b \tau} \sqrt{K}$ , the subsystem (5)-(6) has its unique interior equilibrium  $E = (B^*, H^*) = \left( \frac{r(1 - e^{-d_b \tau})}{2d_b}, \sqrt{K} \right)$  which is always locally asymptotically stable for any delay  $\tau > 0$ .
4. If  $\frac{r}{d_h} > 2e^{d_b \tau} \sqrt{K}$ , the subsystem (5)-(6) has two attractors: the extinction equilibrium  $E_e$  and the interior equilibrium  $E_2 = (B_2^*, H_2^*)$  which are locally asymptotically stable.

### 3.2. Dynamics of the full system

First, we look at the equilibria of Model (2)-(3) by setting  $\frac{dB}{dt} = \frac{dH}{dt} = \frac{dM}{dt} = 0$ . We obtain the subsequent equations:



Equilibrium	Existence	Stability
$E_{00}$	Always	LAS and GAS if $d_h > \frac{re^{-d_b\tau}}{2\sqrt{K}}$
$E_{B^*H^*}$	$d_h = \frac{re^{-d_b\tau}}{2\sqrt{K}}$	LAS
$E_{B_1^*H_1^*}$ and $E_{B_2^*H_2^*}$	$d_h < \frac{re^{-d_b\tau}}{2\sqrt{K}}$	$E_{B_1^*H_1^*}$ is unstable and $E_{B_2^*H_2^*}$ is LAS

Table 2: Summary dynamics of Model (5)-(6) where LAS- Locally Asymptotically Stable; GAS-Globally Asymptotically Stable.

$$\frac{rH^2}{K+H^2} - \frac{\alpha_b BM}{a+B} - d_b B - \frac{rH^2}{K+H^2} e^{-(d_b + \frac{\alpha_b M}{a+B})\tau} = 0 \quad (9a)$$

$$\frac{rH^2}{K+H^2} e^{-(d_b + \frac{\alpha_b M}{a+B})\tau} - \frac{\alpha_h HM}{a+H} - d_h H = 0 \quad (9b)$$

$$\frac{c\alpha_b BM}{a+B} - d_m M = 0 \quad (9c)$$

From equations (9a) - (9c), we know that if  $\tau = 0$ , then System (2)-(3) has only the trivial boundary equilibrium  $E_{000} = (0, 0, 0)$ . And if  $d_h < \frac{re^{-d_b\tau}}{2\sqrt{K}}$ , then Model (2)-(3) has the following two boundary equilibria:

$$E_{B_1^*H_1^*0} = (B_1^*, H_1^*, 0), \quad \text{and} \quad E_{B_2^*H_2^*0} = (B_2^*, H_2^*, 0)$$

where  $B_i^*$  and  $H_i^*$ ,  $i = 1, 2$  are shown in (8) and (7) with  $H_1^* \leq H_2^*$ . For the convenience of the reader, we show their expressions as follows:

$$B_i^* = \frac{d_h[e^{d_b\tau} - 1]}{d_b} H_i^*,$$

and

$$H_i^* = \frac{e^{-d_b\tau} \left( d_b r \pm \sqrt{(d_b r)^2 - 4d_b^2 d_h^2 K e^{2d_b\tau}} \right)}{2d_b d_h}.$$

We have the following theorem regarding the stability of these boundary equilibria:

**Theorem 3.2.** [Boundary equilibria dynamics] Model (2)-(3) always have the extinction equilibrium  $E_{000}$  which is always locally asymptotically stable. If  $d_h < \frac{re^{-d_b\tau}}{2\sqrt{K}}$  Model (2)-(3) has additionally two boundary equilibria  $E_{B_1^*H_1^*0}$  and  $E_{B_2^*H_2^*0}$  where  $E_{B_1^*H_1^*0}$  is always unstable. The equilibrium  $E_{B_2^*H_2^*0}$  is however locally asymptotically stable when  $d_m > \frac{c\alpha_b B_2^*}{a+B_2^*}$  and unstable when  $d_m < \frac{c\alpha_b B_2^*}{a+B_2^*}$ .

**Notes:** By comparing the local stability condition of the equilibrium  $E_{B_2^*H_2^*0}$  of Model (2)-(3) to the local stability condition of the equilibrium  $E_{B_2^*H_2^*}$  of Model (5)-(6) (see Table 2), it implies

that parasitism with smaller mortality rates, e.g.,  $d_m < \frac{\alpha_b B^*}{a+B^*}$ , can destabilize the full system such that  $E_{B^*H^*0}$  becomes unstable. The destabilization of introducing parasitism  $M$  into the honeybee colony has been observed in simulations as well (see Figure 2 in the next section). Now we focus on the global stability of the extinction equilibrium  $E_{000}$  of Model (2)-(3) as follows:

**Theorem 3.3.** [Global stability of full system (2)-(3)]. *If  $d_h > \frac{re^{-d_b\tau}}{2\sqrt{K}}$  and  $d_m > \alpha_b$ , the extinction equilibrium  $E_{000} = (0, 0, 0)$  is globally asymptotically stable.*

**Notes:** Theorem 3.3 indicates that the large mortality rate of honeybee  $d_h$  and mite  $d_m$  can lead to the colony collapsing. Next, we focus on the existence of interior equilibria of Model (2)-(3) that could lead to the colony survival.

Model (2)-(3) has no interior equilibria when  $\tau = 0$ . Therefore, the existence of interior equilibria requires the delay  $\tau > 0$ . Our aim is to find sufficient condition such that Model (2)-(3) has interior equilibria that can lead to the survival of the honeybee colony. To begin our analysis, note that from Equation (9c),  $B^* = \frac{a}{\frac{\alpha_b}{d_m} - 1} > 0$ , that is, the inequality  $\frac{\alpha_b}{d_m} > 1$  is required. Then using equation (9a) and (9b), we obtain follows:

$$\frac{rH^2}{K+H^2} - \frac{\alpha_b BM}{a+B} - d_b B = \frac{\alpha_h HM}{a+H} + d_h H. \quad (10)$$

Let  $f_1(H) = \frac{rH^2}{K+H^2}$  and  $f_2(H) = \frac{B\left(\frac{\alpha_b M}{a+B} + d_b\right)}{1 - e^{-\left(\frac{\alpha_b M}{a+B} + d_b\right)\tau}}$ , where  $B = B^*$ ,  $M = \frac{\frac{rH^2}{K+H^2} - d_b B^* - d_h H}{\frac{\alpha_h H}{a+H} + \frac{\alpha_b B^*}{a+B^*}}$ , and

$$Q(H) = -d_h H^3 + (r - B^* d_b) H^2 - d_h K H - d_b K B^*, \quad (11)$$

with two positive critical points:

$$H_1^c = \frac{(r - d_b B^*) - \sqrt{(r - d_b B^*)^2 - 3K d_h^2}}{3d_h}, \quad H_2^c = \frac{(r - d_b B^*) + \sqrt{(r - d_b B^*)^2 - 3K d_h^2}}{3d_h},$$

if  $d_h < \frac{r - B^* d_b}{\sqrt{3K}}$ . Sufficient conditions for the existence of an interior equilibrium of Model (2)-(3) is provided in Theorem 3.4 as follows:

**Theorem 3.4** (Existence of interior equilibria). *Let  $a, \alpha_b, \alpha_h, c, K, r, d_b, d_h, d_m$  and  $\tau$  be positive parameters. Assume  $\frac{\alpha_b}{d_m} > 1$ ,  $d_h < \frac{r - B^* d_b}{\sqrt{3K}}$  and  $Q(H_2^c) > 0$ . Then  $Q(H)$  has two positive roots  $H_1^r$  and  $H_2^r$  ( $H_1^r < H_2^r$ ), and Model (3) has at least one interior equilibria  $E_{B^*H^*M^*} = (B^*, H^*, M^*)$  with  $B^* = \frac{a}{\frac{\alpha_b}{d_m} - 1}$  when  $\tau \in (\beta_1, \beta_2)$ , where*

$$\beta_1 = \frac{1}{d_b} \ln \left( \frac{f_1(H_2^r)}{f_1(H_2^r) - B^* d_b} \right), \quad \beta_2 = \frac{1}{d_b} \ln \left( \frac{f_1(H_1^r)}{f_1(H_1^r) - B^* d_b} \right).$$

In addition, if  $d_h$  is small sufficiently such that

$$d_h < \frac{(r - B^* d_b) \sqrt{2(r - B^* d_b)}}{3\sqrt{K(r - B^* d_b)} + 3d_b K B^*}$$

then  $Q(H_2^c) > 0$ .

**Notes.** Theorem 3.4 implies that even if the Model (2)-(3) is biologically relevant such that  $\frac{c\alpha_b}{d_m} > \frac{ad_b+r}{r} > 1$  and the queen's egg production is sufficiently large satisfying  $r > d_b B^*$ , Model (2)-(3) may have no interior equilibrium unless the conditions  $Q(H_2^c) > 0$ ,  $f_2(H_1^*) > f_1(H_1^*)$  and  $f_2(H_2^*) < f_1(H_2^*)$  are satisfied in which case a unique interior equilibrium emerges. The expressions of the interior equilibria are too complicated to solve. Thus we need to seek help from numerical simulations to explore the stability of the interior equilibrium.

#### 4. Effects of parasitism and seasonality

In this section, we focus on the dynamical effects of parasitism and seasonality on the colony survival. To explore the effects of parasitism  $M$ , we compare the typical long term dynamics of System (2)-(3) when  $M(0) = 0$  and  $M(0) > 0$  through simulations. Figure 2 shows that (1) When  $M(0) = 0$ , the honeybee colony has equilibrium dynamics and the colony can survive; while (2)  $M(0) = 1$ , we can see that both honeybee and mites coexist through oscillating dynamics. Thus, we could deduce that the introduction of mites (i.e.  $M > 0$ ) can have a destabilizing effect on the system and produce fluctuating dynamics of the honeybee population (brood and adult bees) and mites when the time delay  $\tau$  is large enough. For these simulations, we are using  $\tau = 21$  which correspond to the time it takes for an egg to become an adult bee. We would like to point out that varying  $\alpha_b$  (i.e. the parasitism rate on brood) has a potential to destabilize the dynamics thus drive the population through oscillating dynamics (see Figures 12 and 13 in Appendix B).

#### Long term dynamics of Model (2)-(3) with $M = 0$ and $M > 0$

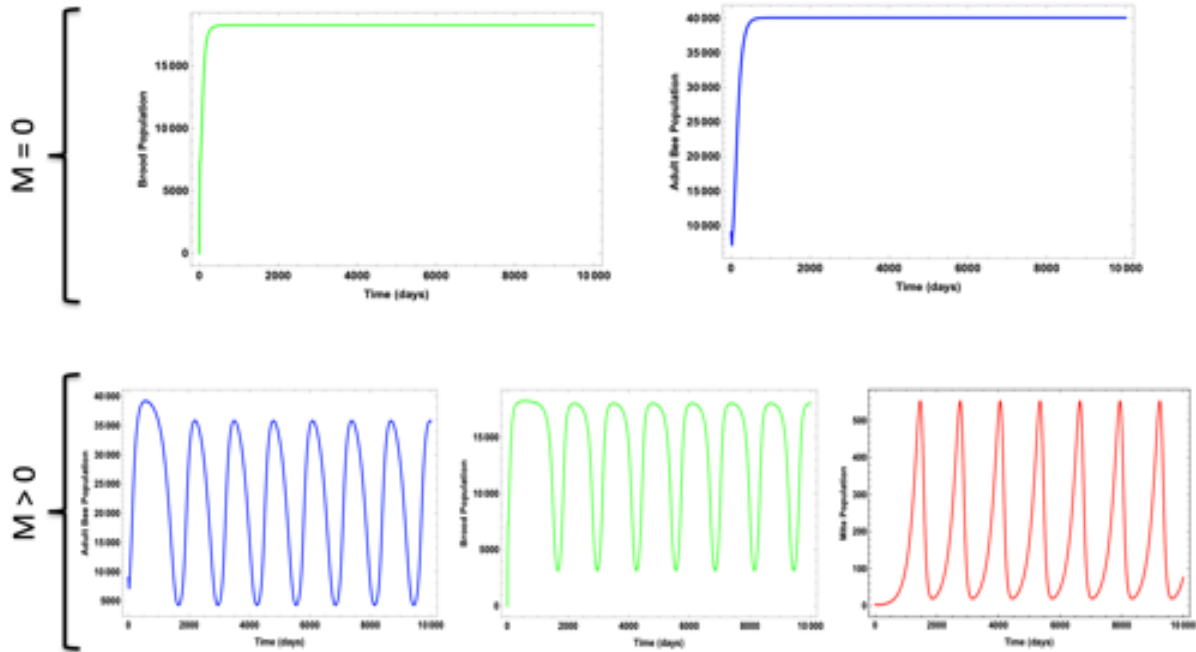


Figure 2: Time series of the brood, adult bee, and mite population using  $\tau = 21$ ,  $r = 1500$ ,  $K = 95000000$ ,  $d_b = 0.051$ ,  $d_h = 0.0121$ ,  $d_m = 0.027$ ,  $\alpha_b = 0.024$ ,  $\alpha_h = 0.8$ ,  $c = 1.9$ ,  $a = 8050$ ,  $\tau = 21$ ,  $B_0(t) = B(0) = 0$ ,  $H(0) = 9000$ , and  $M(0) = 3$ .

**Effects of delay with parasitisms:** From Theorem 3.4, we can check that there is a unique interior equilibrium when we take parameter values as  $r = 1500$ ,  $K = 95000000$ ,  $d_b = 0.051$ ,  $d_h = 0.0121$ ,  $d_m = 0.027$ ,  $\alpha_b = 0.024$ ,  $\alpha_h = 0.8$ ,  $c = 1.9$ ,  $a = 8050$ . Let us take initial conditions  $B_0(t) = B(0) = 0$ ,  $H(0) = 9000$ , and  $M(0) = 3$  and vary the maturation time  $\tau \in (0, 26]$  in Figure 3. Then we have the following dynamics:

with  $\tau = 15$ ,  $E_{B^*H^*M^*} = (11\ 685.5, 16\ 727.2, 579.905)$ ; **stable** equilibrium (see Fig. 3(a)-(c))

with  $\tau = 21$ ,  $E_{B^*H^*M^*} = (11\ 685.5, 12\ 102.5, 338.558)$ ; **periodic** solutions (see Fig. 3(d)-(f))

with  $\tau = 26$ ,  $E_{B^*H^*M^*} = (11\ 685.5, 10\ 607.8, 189.793)$ ; **unstable** equilibrium (see Fig. 3(g)-(i))

These simulations suggest that as  $\tau$  increases, ( $0 < \tau < 16$ ), the interior equilibrium is asymptotically stable with our choice of parameter values above. Then, for  $16 < \tau < 26$ , the system has periodic solutions which could be due to a possible Hopf bifurcation. Lastly, for  $\tau > 26$  the interior equilibrium becomes unstable with a large oscillating cycle that hits the stable manifold of the extinction equilibrium  $E_{000}$  such that both honeybee and mite populations die out.

### Delay effects on Model (2)-(3) long term dynamics

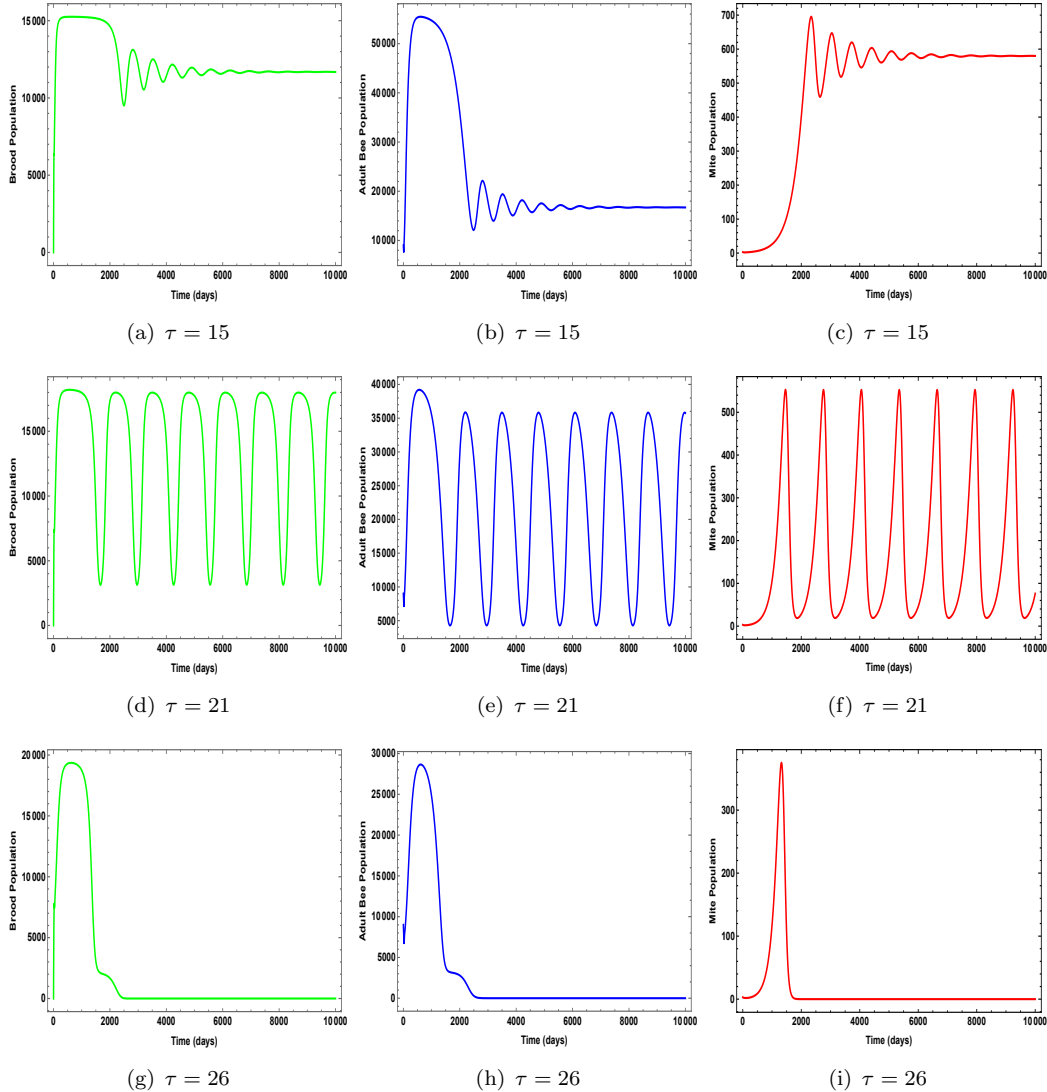


Figure 3: Time series of the brood, adult bee, and mite population using  $r = 1500$ ,  $K = 95000000$ ,  $d_b = 0.051$ ,  $d_h = 0.0121$ ,  $d_m = 0.027$ ,  $\alpha_b = 0.024$ ,  $\alpha_h = 0.8$ ,  $c = 1.9$ ,  $a = 8050$ , with I.C.  $B(0) = 0$ ,  $H(0) = 9000$ , and  $M(0) = 3$ .

#### 4.1. Data and Seasonality

The data consists of the population of honeybees, *Varroa* mites, and brood in colonies collected in Casa Grande, at the University of Arizona West Agricultural Facility (20 colonies). The data were established in desert climate of Arizona where temperatures are favorable for bees foraging activity, especially, during April until November (when the data were collected). All colonies initially had 9000 package bees with a queen and miticide treatment was used to control the *Varroa* population in the nearby apiaries at the beginning of the experiment (April of 2014).

In order to approximate the honeybee and brood population data in the colonies, frames of bees were measured monthly from May to November using a method from [16]. This method consist of

estimating brood and bees on an area of the frames using a 5 cm  $\times$  5 cm grid that cover the entire side of the comb. Note that one frame of bees contains approximately 2506 bees and 5200 brood cells [16] and maximum availability of brood on frame occurs at 80% (i.e. only 80% of frames are cover with brood at the most). Thus the colony of bees are estimated by computing: frames of bees  $\times$  2506, and colony of brood are estimating as: frames of brood  $\times$  0.8  $\times$  5200. The *Varroa* mite population density in the colonies were also collected from May until November. During the experiment season (i.e. May to November), 300 bees were brushed into a jar then the number of mites on the 300 bees were counted monthly and these constitute the phoretic mites. The population of the reproductive mites were also estimated by counting the total number of mites per sampled cells. The total mite population in a colony is hence the sum of the phoretic and reproductive mite. We proceed as follow to find the estimated mite population in colonies. Recall that the number of phoretic mites obtained is the mites per 300 bees. Then, the calculation of the phoretic mite population per colony are estimating by:  $\frac{\text{mites per 300 bees}}{300} \times \text{population of bees per colony}$ . We calculated the reproductive mites per colony by performing  $\frac{\text{total number of mites} \times 5200}{\text{number of cells sampled}}$ . The sum of the phoretic mites and reproductive yield the total population per colonies. DeGrandi-Hoffman et al. [13] follow similar approach to estimate the population of bees, brood, and mite per colony.

Now we note that the number of eggs laid by the queen bee is a function of the ambient temperature, photoperiod, and adult population in the colony [15]. In addition, it has also been shown that the total number of daily eggs laid by the queen is a decreasing function of the number of days the queen has been laying eggs [15], i.e., older queens laid approximately less eggs comparatively to younger queens. Given that number of eggs laid by the queen is temperature and photoperiodic dependent (i.e. changed seasonally), the egg-laying rate must hence be described by a periodic function. It is well known that any periodic function can be represented as an infinite sum of sines and cosines [23]. In order to keep our model simple and tractable, we combine these factors (i.e. temperature, photoperiod, etc.) and adapt the first order harmonic function presented in [23] to our egg-laying rate  $r_1$  and  $r_2$  in Model (2) and (3) to obtain:

$$r_1 = r \left[ 1 + \cos \left( \frac{2\pi(t - \Phi)}{365} \right) \right] \quad \text{and} \quad r_2 = r \left[ 1 + \cos \left( \frac{2\pi(t - \tau - \Phi)}{365} \right) \right] \quad (12)$$

where  $\Phi$  denote the day of the year with the maximum eggs laying rate,  $r$  is the baseline egg-laying rate from [20, 60], and  $t$  is the time measure in days. Using Equation (12), we obtain the number of eggs laid by the queen over a period of a year as depicted in Figure 4.

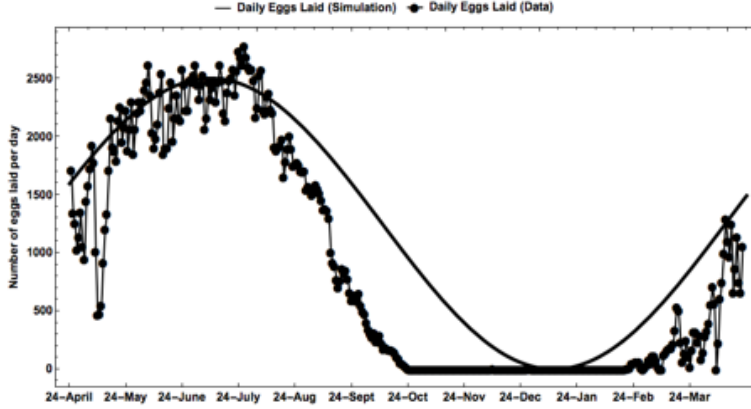


Figure 4: Number of eggs laid by a strong full mated queen without a constraint over a period of one year following Equation (12) with  $r = 1250$  and  $\Phi = 75$  ( $\approx$  July 8). The data was simulated using the BEEPOP model from [15] by taking into account daily temperature, photoperiod, and adult population in the colony.

Using *Varroa* mites and honeybees life history parameters in the ranges provided in Table 1, we estimated the parameters  $\alpha_b$ ,  $\alpha_h$ ,  $a$  without considering seasonality ( $\alpha_b = 0.045$ ,  $\alpha_h = 0.49$ , and  $a = 8500$ ) and in the presence of seasonality ( $\alpha_b = 0.0447$ ,  $\alpha_h = 0.8$ , and  $a = 8050$ ). To illustrate the importance of seasonality when modeling the dynamics of honeybee and mite population, we present the best fit without seasonality in Figures 5 and the best fit with seasonality in Figures 6 using the egg-laying rate function in (12).

- **Best fit without seasonality:**

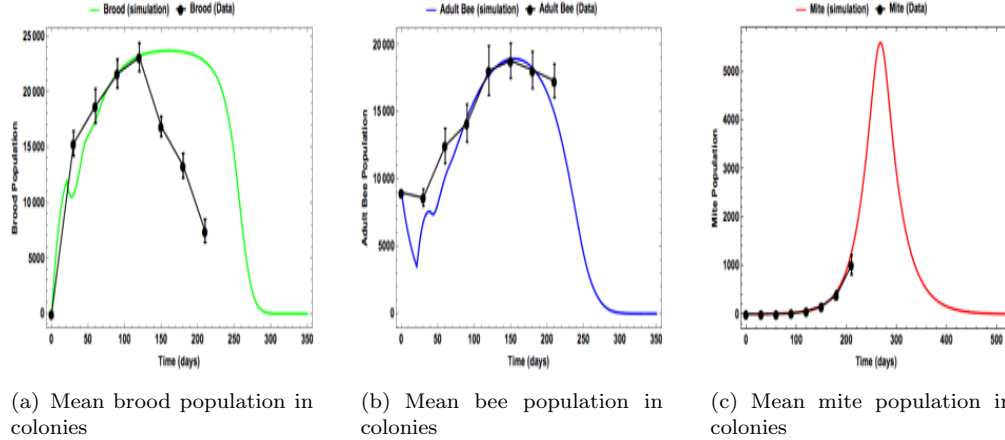


Figure 5: Time series of the brood, adult bee, and mite model simulation together with the average population data in Casa Grande. These figures represent respectively the average brood, adult bee, and mite population of 20 colonies with its standard error. The simulation is performed using  $r = 1500$ ,  $K = 35000000$ ,  $d_b = 0.0185$ ,  $d_h = 0.045$ ,  $d_m = 0.029$ ,  $\alpha_b = 0.045$ ,  $\alpha_h = 0.49$ ,  $c = 1.9$ ,  $a = 8500$ ,  $\tau = 21$ ,  $B_0(t) = B(0) = 0$ ,  $H(0) = 9000$ , and  $M(0) = 3$ . Time  $t = 0$  corresponds to April 24.

- **Best fit with seasonality:**

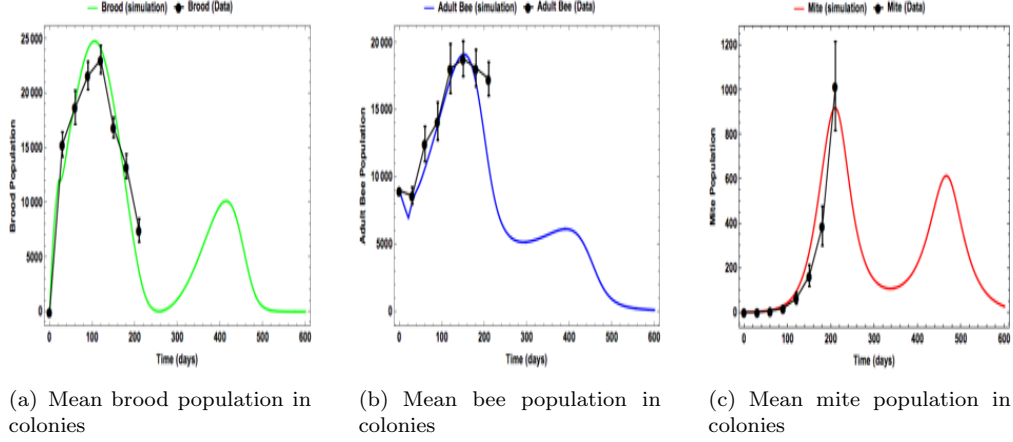


Figure 6: Time series of the brood, adult bee, and mite model simulation together with the average population data in Casa Grande. These figures represent respectively the average brood, adult bee, and mite population of 20 colonies with its standard error. The simulation is performed using using  $r = 1500$ ,  $K = 95000000$ ,  $d_b = 0.051$ ,  $d_h = 0.0121$ ,  $d_m = 0.027$ ,  $\alpha_b = 0.0447$ ,  $\alpha_h = 0.8$ ,  $c = 1.9$ ,  $a = 8050$ ,  $\Phi = 65$ ,  $\tau = 21$ ,  $B_0(t) = B(0) = 0$ ,  $H(0) = 9000$ , and  $M(0) = 3$ . Time  $t = 0$  corresponds to April 24.

### Comparisons between the best fit with and without seasonality (Figures 5 and 6) :

1. A better fit of the model simulation to the data is obtained when seasonality is taken into account in Figure 6 as oppose to Figure 5. This reflects a more realistic life history parameter of honeybees and mites as presented in Figure 6.
2. The parameter values used for both with and without seasonality produce the following equilibrium points on Model (2)-(3):

$$E_{000} = (0, 0, 0), \quad E_{B_1^*H_1^*0} = (24171, 20930.2, 0), \quad E_{B_2^*H_2^*0} = (1931.15, 1672.22, 0)$$

We highlight that under these parameter values, the sufficient conditions in Theorem 3.4 for the existence of interior equilibrium are not satisfied, thus, there is no interior point. According to Theorem 3.2,  $E_{000}$  and  $E_{B_1^*H_1^*0}$  are asymptotically stable while  $E_{B_2^*H_2^*0}$  is unstable. Given initial conditions in the simulations shown in Figures 5(a)-5(c), honeybee and mite population go extinct as  $t \rightarrow \infty$ . But for other initial conditions, we could have the survival of the honeybee only.

3. The population of brood, adult bees, and mites are driven extinct without seasonality in approximately 350, 350, and 500 days, respectively, and in approximately 600, 600, 600 days, respectively, with seasonality. This result indicates that the environmental changes due to seasonality could promote a longer survival of honeybee colony infested by the *Varroa* mites. This highlights the effects of seasonal fluctuation on survivability of species.
4. In the presence of seasonality, the population of brood, adult bee, and mite tend to have a second rise (after approximately one year) and this is due to the cycle of the egg-laying rate by the queen illustrated in Figure 4 (see the second pick starting in February 24).



**Effects of  $\alpha_b$  and seasonality:** In Appendix B, we provide comparison on the role of  $\alpha_b$  on the population dynamics of brood, adult bee, and mite in Figures 7, 12, 13, and 14. Those simulations show time series simulations and comparison of the dynamics with and without seasonality under different  $\alpha_b$  values. For these simulations, parameters were chosen such that a unique interior equilibrium exist and is locally stable. For the smallest value of  $\alpha_b$ , (i.e. when the unique interior equilibrium is stable without seasonality and  $\alpha_b = 0.022$ ), taking seasonality into account drive the mite population to die out while the adult bee population stabilize and the brood population fluctuate (Figure 7). An intermediate value of  $\alpha_b = 0.024$  has the potential to generate fluctuating dynamics without seasonality while only the mite population die out when seasonality is considered (Figure 12). In the presence of seasonality, a larger  $\alpha_b$  (i.e. 0.027) has the potential to drive the brood, adult bee, and mite through non-periodic dynamics while all population dies out without seasonality (Figure 13). Large value of  $\alpha_b = 0.028$  has the ability to drive colonies to collapse irrespective to seasonality (Figure 14). While colonies can collapse under large  $\alpha_b$  and in the absence of control measure, the results presented in Figure 14 display the fact that all population dies out before before the third year (1000<sup>th</sup> day) when seasonality is not taking into account and the populations persist over four years under seasonality. Such result highlights the importance of considering seasonality when modeling the population dynamics of honeybee under infestation by *Varroa* mite.

## 4.2. Sensitivity Analysis

Data fitting and parameter estimation with and without seasonality of  $\alpha_b$ ,  $\alpha_h$ , and  $a$  are provided in Section 4.1 using colonies' data from [16] (see Figure 5 for fitting without seasonality and Figure 6 for fitting with seasonality) and all other parameters sources are listed in Table 1. It is often noted in mathematical biology that natural variation, error in measurements may cause a variation in the parameter of the system [42]. Thus, identifying critical inputs parameters of a model and quantifying how the uncertainty of such parameters impact model outcome is paramount. This section measures and quantify the effect of parameter sensitivity on the population size of brood, adult bee, and mite, respectively, through global sensitivity analysis (SA). As noted by [42], different SA techniques will perform better for specific types of mathematical and computational models, and there has been numerous global sensitivity methods discussed in the literatures (see [8, 32, 33, 56] for a detail review on Monte Carlo analysis and variance decomposition methods). However, in order to obtain a holistic view regarding the sensitivity of the input parameters on the model outcome, two different SA methods were employed: (1) the Partial Rank Correlation Coefficient (PRCC) SA with Latin Hypercube Sampling (or LHS first introduced by [44]) as the sampling technique; (2) and the Extended Fourier Amplitude Sensitivity Test (eFAST). We followed the methodology discussed in [42] for both SA methods (i.e. LHS/PRCC and eFAST).

For our analysis, SA was conducted on the time corresponding to the largest population size in Figure 6 as output and the eleven parameters of Model (2)-(3) when seasonality is taken into account (i.e. we used the eggs laying rate formula (12)). The time corresponding to the largest population size was selected to determine how the input parameters may affect the brood, adult bee, and mite population at their peak thus maintaining or causing the collapse of the colony. The result of the SA are presented in Figures 8, 9, and 10 for the brood, adult honeybee and mite

population.

Both PRCC and eFAST values in Figure 8 indicate that  $r$ ,  $d_b$ , and  $K$  are the most sensitive parameters affecting the brood population size with  $r$  (the maximum queen’s egg-laying rate) being the most sensitive of the three. The PRCC values of  $\Phi$  and  $d_h$  in Figure 8(b) appear to be at the intermediate level ( $\approx 0.5$  as shown in Table 3 in Appendix B). The parameters  $d_m$ ,  $\alpha_b$ ,  $\alpha_h$ ,  $a$ , and  $c$  are shown not to have a high sensitivity value in both Figures 8(a) and 8(b) suggesting that the largest brood population size is not sensitive to mite infestation rate but rather the queen’s ability to lay eggs, which is a function of seasonality, age of the queen, nutrition, etc. [15]. It is observable in Figure 9 and 10 that the most sensitive parameter affecting the adult bee and mite population size from both the PRCC and eFAST indexes are  $r$ ,  $\alpha_b$ , and  $c$  with  $d_h$  having a high PRCC value in Figure 9(b). Moreover, the input parameters  $d_b$  and  $d_m$  are shown to have a high sensitivity on the mite population from both the PRCC and eFAST indexes (Figure 10) indicating that reduction of the mite mortality through proper control measure may release parasitic pressure on the colony. It is significant to point out that the maximum queen’s egg-laying rate,  $r$ , appears to be the most sensitive parameter affecting the population size of the brood, adult honeybee (i.e. the entire colony of honeybee), and mite under both PRCC and eFAST SA methods (Figures 8, 9, and 10). Such result has been confirmed by [15] where the authors stated that the queen’s egg-laying potential has the greatest effect on colony population size. It is also noticeable that the natural mortality of adult bee (i.e.  $\alpha_h$ ) is not very sensitive with a low PRCC and eFAST indexes for the brood, adult bee, and mite population. The SA also reveals that the infestation rate on the brood (i.e.  $\alpha_b$ ) may be another important parameter affecting the population size of the colony (see high PRCC and eFAST indexes values in Table 4 and 5 in Appendix B). Our discussion continues by exploring the role of  $\alpha_b$  on the population dynamics.

## 5. Discussion

Colonies of honeybees have started to see a sudden decline over the last decade [40]. While the direct cause of this collapse may not be trivial, it is argue that there are a combination of stresses involve in the loss of colonies worldwide [30, 40]. The presence of *Varroa* mite was strongly shown to be one of the causing phenomenon behind colonies’ collapse [14, 35, 45]. In this study, we proposed a nonlinear stage structure delay differential equations that describes the interactions between brood, adult honeybees, and mites in a single patch framework where the maturation from brood to adult honeybee was taken into account. Moreover, noting that the temporal dynamics of honeybee colonies varies with respect to seasonality (e.g. temperature, photoperiod, etc.) [15], seasonality is incorporated into our model and proper comparisons are made between the model with and without seasonality. The theoretical results combined with numerical simulations provide useful insights on how the presence of mites affect the dynamical outcomes of the adult honeybee and brood population respectively. More specifically, our work suggest the following:

Theorem 3.1 provides the positivity and boundedness condition of Model (2)-(3). In addition, Theorem 3.2 and Theorem 3.3 in the paper of Chen et al. [34] provide sufficient conditions for the existence and stability of the boundary equilibria  $E_{B_1^*H_1^*0}$  and  $E_{B_2^*H_2^*0}$  of the system, thus illustrating the dynamics that may prone a mite-free colony. It follows from this result that initial

population size play an important role in sustaining a healthy bee colony. Moreover, small natural death rate of adult bee population may promote a coexistence of brood and adult bee in a mite-free colony. Nonetheless, an introduction of mites into a mite-free colony has the ability to drive all populations (i.e. brood, adult bee, and mite) through a fluctuating dynamics (see Figure 2) thus showing the effect of mite population on colony dynamics. Delay also the ability to stabilize, destabilize, or even promotes a fluctuating dynamics, leading to the coexistence or death of all species (Figures 3(a)-3(i)). Theorem 3.4 provides sufficient conditions on the existence of the unique interior equilibrium of Model (2)-(3). Through numerical simulations, we showed possible dynamics that may drive all populations to coexist at the interior equilibrium  $E_{B^*H^*M^*}$  when seasonality is not considered (see simulation without seasonality in Figure 3 and 7). Incorporating seasonality under the same life history parameter values of the system, when all population coexist, has the ability to drive mite population to die out while the adult bee population stabilize at an equilibrium and the brood population goes through fluctuating dynamics (see with and without seasonality Figure 7). Also, a better representation of the model to the data can be observed in Figure (6) as oppose to Figure (5) when seasonality was taken into account, thus exemplifying more realistic life history parameters of the brood-adult bee-mite system when seasonality is incorporated in the system.

The results from the sensitivity analysis in Figures 8, 9, and 10 show that the queen's egg-laying rate has the highest impact on the colony's population, which supports the work of [15]. Both our PRCC and eFAST method agree with the latter result. The infestation rate on the brood population was also noted as another important parameter affecting the colony's population size. Results from the time series simulations in Figures 7, 12, 13, and 14 illustrate the dynamics generated by the mite to brood infestation rate on the population size with and without seasonality. When seasonality is not taken into account, small infestation on the brood could promote coexistence of all species at the interior equilibrium, intermediate infestation rate could yield the coexistence of all species through fluctuating dynamics, and large infestation rate could drive the colony to collapse. However, by incorporating seasonality, our results show that mite population could die out under small and large infestation rate but all the population may go through non-periodic dynamics under an intermediate infestation rate on the brood (Figures 7, 12, 13, and 14). Moreover, by comparing the seasonal and non-seasonal dynamics in Figures 7-14, our results indicate that in the environment where high seasonal fluctuation is present, infested colonies may survive longer than in an environment when small or no fluctuation is observed. These findings highlight the importance of seasonality in the honeybee interaction with *Varroa* mite and some of the parameters that may promote a mite-free colony or drive the colony to collapse. It will be interesting to study similar dynamics when honeybee population are prone to use a defensive mechanism such as a grooming behavior. This will be subject to a future study.

## Appendix A: Proofs

### Proof of Theorem 3.1

*Proof.* 1. We will proceed by first showing the positivity of our system. First, we prove that  $B(t) > 0, H(t) > 0, M(t) > 0$  for all  $t \in [0, \tau]$ . On the contrary, we assume that there exists  $t_0 \in (0, \tau]$  such that  $B(t_0) = 0$  and  $B(t) > 0$  for  $t \in (0, t_0)$ . Then we have from the first

equation of (2) that

$$\frac{dB}{dt} \geq -\alpha_b \frac{B}{a+B} M - d_b B - e^{-\int_{t-\tau}^t [d_b + \frac{\alpha_b M(s)}{a+B(s)}] ds} B_0(t-\tau), \quad t \in (0, t_0).$$

Integrating from 0 to  $t_0$ , we have

$$B(t_0) e^{\int_0^{t_0} [d_b + \frac{\alpha_b M(s)}{a+B(s)}] ds} - B(0) \geq - \int_0^{t_0} e^{-\int_{t-\tau}^0 [d_b + \frac{\alpha_b M(s)}{a+B(s)}] ds} B_0(t-\tau) dt. \quad (13)$$

Substituting (4) into (13), we get

$$\begin{aligned} \int_{-\tau}^0 B(t_0) e^{-\int_t^0 [d_b + \frac{\alpha_b M_0(s)}{a+B_0(s)}] ds} dt &\leq \int_0^{t_0} e^{-\int_{t-\tau}^0 [d_b + \frac{\alpha_b M(s)}{a+B(s)}] ds} B_0(t-\tau) dt \\ &= \int_{-\tau}^{t_0-\tau} e^{-\int_t^0 [d_b + \frac{\alpha_b M_0(s)}{a+B_0(s)}] ds} B_0(t) dt, \end{aligned}$$

which is a contradiction since  $t_0 - \tau < 0$  and  $B_0(t) > 0, t \in [-\tau, 0]$ . Therefore,  $B(t) > 0$  for all  $t \in [0, \tau]$ .

If there exists  $t_0 \in (0, \tau]$  such that  $H(t_0) = 0$  and  $H(t) > 0$  for  $t \in (0, t_0)$ . Then  $H'(t_0) \leq 0$ . By the second equation of (2), we get a contradiction that

$$0 \geq H'(t_0) = e^{-\int_{t_0-\tau}^{t_0} [d_b + \frac{\alpha_b M(s)}{a+B(s)}] ds} B_0(t_0 - \tau) > 0$$

since  $B_0(t) > 0, t \in [-\tau, 0]$ . Therefore,  $H(t) > 0$  for all  $t \in [0, \tau]$ . Furthermore, the third equation of (2) implies that

$$M(t) = M(0) e^{-\int_0^t [d_m - \frac{c\alpha_b B(s)}{a+B(s)}] ds} > 0, \quad t \in [0, \tau].$$

Now, we show by induction that both  $B(t), H(t)$  and  $M(t)$  are positive on  $n\tau \leq t \leq (n+1)\tau, n = 0, 1, \dots$ . We have proved that it is valid for  $n = 0$ . We only show that it is also valid for the case  $n = 1$ . For  $n \geq 2$ , it can be dealt with similarly. On the contrary, we assume that there exists  $t_0 \in (\tau, 2\tau]$  such that  $B(t_0) = 0$  and  $B(t) > 0$  for  $t \in (0, t_0)$ . Then by the first equation of (3), we have

$$\frac{dB}{dt} \geq -\alpha_b \frac{B}{a+B} M - d_b B - e^{-\int_{t-\tau}^t [d_b + \frac{\alpha_b M(s)}{a+B(s)}] ds} \frac{rH^2(t-\tau)}{K + H^2(t-\tau)}, \quad t \in (0, t_0).$$

It follows that

$$\frac{d}{dt} \left( B(t) e^{\int_{\tau}^t [d_b + \frac{\alpha_b M(s)}{a+B(s)}] ds} \right) \geq -e^{-\int_{t-\tau}^{\tau} [d_b + \frac{\alpha_b M(s)}{a+B(s)}] ds} \frac{rH^2(t-\tau)}{K + H^2(t-\tau)}.$$

Integrating from  $\tau$  to  $t_0$ , we get

$$B(t_0) e^{\int_{\tau}^{t_0} [d_b + \frac{\alpha_b M(s)}{a+B(s)}] ds} - B(\tau) \geq - \int_{\tau}^{t_0} e^{-\int_{t-\tau}^{\tau} [d_b + \frac{\alpha_b M(s)}{a+B(s)}] ds} \frac{rH^2(t-\tau)}{K + H^2(t-\tau)} dt. \quad (14)$$

From the first equation of (2) and (4), we have

$$B(\tau) = \int_0^{\tau} e^{-\int_s^{\tau} [d_b + \frac{\alpha_b M(s)}{a+B(s)}] ds} \frac{rH^2(t)}{K + H^2(t)} dt. \quad (15)$$

Substituting (15) into (14), we obtain

$$\begin{aligned} \int_0^\tau e^{-\int_s^\tau \left[ d_b + \frac{\alpha_b M(s)}{a+B(s)} \right] ds} \frac{rH^2(t)}{K+H^2(t)} dt &< \int_\tau^{t_0} e^{-\int_{t-\tau}^t \left[ d_b + \frac{\alpha_b M(s)}{a+B(s)} \right] ds} \frac{rH^2(t-\tau)}{K+H^2(t-\tau)} dt \\ &= \int_0^{t_0-\tau} e^{-\int_s^\tau \left[ d_b + \frac{\alpha_b M(s)}{a+B(s)} \right] ds} \frac{rH^2(s)}{K+H^2(s)} ds, \end{aligned}$$

which is contradiction since  $t_0 - \tau < \tau$  and  $H(t) > 0, t \in [0, \tau]$ . Therefore,  $B(t) > 0$  for all  $t \in [0, 2\tau]$ .

Similar to the arguments for case  $t \in (0, \tau]$ , it is easy to verify that  $H(t)$  and  $M(t)$  are positive on  $\tau \leq t \leq 2\tau$ . Furthermore, we can get by induction that  $B(t) > 0, H(t) > 0, M(t) > 0$  for all  $t > 0$ .

2. We now proceed with the boundedness of our system in below. Define  $W = cB + cH + M$ , then we have

$$\begin{aligned} \frac{dW}{dt} &= c \frac{dB}{dt} + c \frac{dH}{dt} + \frac{dM}{dt} \\ &= \frac{crH^2}{K+H^2} - \frac{c\alpha_b HM}{a+H} - cd_b B - cd_h H - d_m M \\ &\leq \frac{crH^2}{K+H^2} - cd_b B - cd_h H - d_m M \\ &\leq cr - \min\{d_b, d_h, d_m\}(cB + cH + M) = cr - \min\{d_b, d_h, d_m\}W. \end{aligned}$$

Therefore, we have

$$\limsup_{t \rightarrow \infty} W(t) = \limsup_{t \rightarrow \infty} (cB(t) + cH(t) + M(t)) \leq \frac{cr}{\min\{d_b, d_h, d_m\}}.$$

□

### Proof of Theorem 3.2

*Proof.* As  $M = 0$ , model (3) reduces to the model of Chen et al., then the existence of the boundary equilibria can be obtained directly by Proposition 3.1 in their paper [34]. We proceed with the stability of the boundary equilibria  $E_{000}$ ,  $E_{B_1^* H_1^* 0}$ , and  $E_{B_2^* H_2^* 0}$  by linearizing our system. First, we note that  $E_{B_1^* H_1^* 0}$  is unstable since  $E_{B_1^*, H_1^*}$  is unstable in the model of Chen et al. by Theorem 3.3 [34]. So, we only consider the stability of  $E_{000}$  and  $E_{B_2^* H_2^* 0}$ .

To facilitate our analysis, we introduce the variable  $P(t) = e^{-\int_{t-\tau}^t \left( d_b + \frac{\alpha_b M(s)}{a+B(s)} \right) ds}$  and Model (3) becomes:

$$\begin{aligned} \frac{dB}{dt} &= \frac{rH^2}{K+H^2} - \alpha_b \frac{B}{a+B} M - d_b B - \frac{rPH(t-\tau)^2}{K+H(t-\tau)^2} \\ \frac{dH}{dt} &= \frac{rPH(t-\tau)^2}{K+H(t-\tau)^2} - \alpha_h \frac{H}{a+H} M - d_h H \\ \frac{dM}{dt} &= c\alpha_b \frac{B}{a+B} M - d_m M \\ \frac{dP}{dt} &= \frac{\alpha_b PM(t-\tau)}{a+B(t-\tau)} - \frac{\alpha_b PM}{a+B} \end{aligned} \tag{16}$$

Let  $(B^*, H^*, M^*, P^*)$  be the equilibrium of the system (16) where  $P^* = e^{-\left(d_b + \frac{\alpha_b M^*}{a+B^*}\right)\tau}$ . The linearization matrix of Model (16) at the equilibrium  $(B^*, H^*, M^*, P^*)$  can be represented as follows:

$$\begin{aligned}
D \begin{pmatrix} \dot{B}(t) \\ \dot{H}(t) \\ \dot{M}(t) \\ \dot{P}(t) \end{pmatrix} \Big|_{(B^*, H^*, M^*, P^*)} &= \begin{bmatrix} \frac{-a\alpha_b M^*}{(a+B^*)^2} - d_b & \frac{2rKH^*}{(K+(H^*)^2)^2} & -\frac{\alpha_b B^*}{a+B^*} & -\frac{r(H^*)^2}{K+(H^*)^2} \\ 0 & \frac{-a\alpha_h M^*}{(a+H^*)^2} - d_h & -\frac{\alpha_h H^*}{a+H^*} & \frac{r(H^*)^2}{K+(H^*)^2} \\ \frac{a c \alpha_b M^*}{(a+B^*)^2} & 0 & \frac{c \alpha_b B^*}{a+B^*} - d_m & 0 \\ \frac{\alpha_b P^* M^*}{(a+B^*)^2} & 0 & -\frac{\alpha_b P^*}{a+B^*} & 0 \end{bmatrix} \begin{bmatrix} B(t) \\ H(t) \\ M(t) \\ P(t) \end{bmatrix} \\
&+ \begin{bmatrix} 0 & -\frac{2rKP^*H^*}{(K+(H^*)^2)^2} & 0 & 0 \\ 0 & \frac{2rKP^*H^*}{(K+(H^*)^2)^2} & 0 & 0 \\ 0 & 0 & 0 & 0 \\ -\frac{\alpha_b P^* M^*}{(a+B^*)^2} & 0 & \frac{\alpha_b P^*}{a+B^*} & 0 \end{bmatrix} \begin{bmatrix} B(t-\tau) \\ H(t-\tau) \\ M(t-\tau) \\ P(t-\tau) \end{bmatrix}. \\
&:= U\Phi(t) + V\Phi(t-\tau).
\end{aligned} \tag{17}$$

The characteristic equation of (17) is given by

$$C(\lambda) = \left| \lambda I - U - e^{-\lambda\tau} V \right| = 0.$$

Notice  $P^* = e^{-d_b\tau}$  when  $M^* = 0$ . By a direct computation, we get

$$C(\lambda) = \lambda(\lambda + d_b) \left( \lambda - \frac{c\alpha_b B^*}{a+B^*} + d_m \right) \left( \lambda + d_h - \frac{2rKH^*}{(K+(H^*)^2)^2} e^{-(\lambda+d_b)\tau} \right).$$

which always has eigenvalues  $\lambda_0 = 0$ , which is in the direction  $P$ ,  $\lambda_1 = -d_b < 0$  and  $\lambda_2 = \frac{c\alpha_b B^*}{a+B^*} - d_m$ . The other eigenvalues satisfy the following algebraic equation

$$L(\lambda) := \lambda + d_h - \frac{2rKH^*}{(K+(H^*)^2)^2} e^{-(\lambda+d_b)\tau} = 0. \tag{18}$$

Therefore, the stability of  $E_{000}$  and  $E_{B_2^* H_2^* 0}$  is determined by the signs of  $\lambda_2$  and of the roots of  $L(\lambda) = 0$ .

At extinction equilibrium  $E_{000} = (0, 0, 0)$ ,  $\lambda_2 = -d_m$  and  $L(\lambda) = \lambda + d_h$ , therefore,  $E_0 = (0, 0)$  is locally asymptotically stable for all  $\tau > 0$ .

At  $E_{B_2^* H_2^* 0}$ , from the proof of Theorem 3.3 in the paper of Chen et al. [34] (by Theorem 4.7 of Smith [58]), we know that all roots of  $L(\lambda)$  have negative real parts. Thus, we can conclude that if  $d_m > \frac{c\alpha_b B^*}{a+B^*}$  then  $E_{B_2^* H_2^* 0}$  is locally asymptotically stable, while unstable if  $d_m < \frac{c\alpha_b B^*}{a+B^*}$ .  $\square$

### Proof of Theorem 3.4

*Proof.* Note that from Equation (9c),  $B^* = \frac{a}{\frac{c\alpha_b}{d_m} - 1}$ , and from Equation (9a) and (9b), we obtain

$$\begin{aligned}
\frac{rH^{*2}}{K+H^{*2}} e^{-\left(d_b + \frac{\alpha_b M^*}{a+B^*}\right)\tau} &= \frac{rH^{*2}}{K+H^{*2}} - \frac{\alpha_b B^* M^*}{a+B^*} - d_b B^* \\
\frac{rH^{*2}}{K+H^{*2}} e^{-\left(d_b + \frac{\alpha_b M^*}{a+B^*}\right)\tau} &= \frac{\alpha_h H^* M^*}{a+H^*} + d_h H^*
\end{aligned}$$

which gives

$$\frac{rH^{*2}}{K+H^{*2}} - \frac{\alpha_b B^* M^*}{a+B^*} - d_b B^* = \frac{\alpha_h H^* M^*}{a+H^*} + d_h H^*. \quad (19)$$

Then

$$M^* = \frac{\frac{rH^{*2}}{K+H^{*2}} - d_b B^* - d_h H^*}{\frac{\alpha_h H^*}{a+H^*} + \frac{\alpha_b B^*}{a+B^*}}, \quad (20)$$

From Equation (9a) we have the following:

$$\frac{rH^{*2}}{K+H^{*2}} \left(1 - e^{-\left(d_b + \frac{\alpha_b M^*}{a+B^*}\right)\tau}\right) = B^* \left(d_b + \frac{\alpha_b M^*}{a+B^*}\right) \Leftrightarrow \frac{rH^{*2}}{K+H^{*2}} = \frac{B^* \left(\frac{\alpha_b M^*}{a+B^*} + d_b\right)}{1 - e^{-\left(\frac{\alpha_b M^*}{a+B^*} + d_b\right)\tau}}$$

Let

$$f_1(H^*) = \frac{rH^{*2}}{K+H^{*2}}, \quad \text{and} \quad f_2(H^*) = \frac{B^* \left(\frac{\alpha_b M^*}{a+B^*} + d_b\right)}{1 - e^{-\left(\frac{\alpha_b M^*}{a+B^*} + d_b\right)\tau}}.$$

Thus,  $(B^*, H^*, M^*)$  is a interior equilibria if and only if  $B^* = \frac{a}{\frac{c\alpha_b}{d_m} - 1} > 0$ , i.e.  $\frac{c\alpha_b}{d_m} > 1$ ,  $H^* > 0$  is a positive root of  $f_1(H^*) = f_2(H^*)$  and  $M^*$  defined in (20) is positive.

In what follows, we assume  $\frac{c\alpha_b}{d_m} > 1$ .

Regard  $M^*$  defined in (20) as a function on  $H^*$ , denoted as  $M^*(H^*)$ , we rewrite it as  $M^*(H^*) = \frac{Q(H^*)}{P(H^*)}$ , where

$$Q(H^*) = -d_h H^{*3} + (r - B^* d_b) H^{*2} - d_h K H^* - d_b K B^*, \\ P(H^*) = (K + H^{*2}) \left(\frac{\alpha_h H^*}{a+H^*} + \frac{\alpha_b B^*}{a+B^*}\right).$$

Clearly,  $Q(0) = -d_b K B^* < 0$ ,  $P(0) = K \frac{\alpha_b B^*}{a+B^*}$ , and  $M(0) = -\frac{d_b}{\alpha_b} (a + B^*)$ . Also, for all  $H^* \geq 0$ ,  $P(H^*) > 0$ . Thus, the sign of  $M(H^*)$  is determined by  $Q(H^*)$ .

(i) If  $r - B^* d_b \leq 0$ , then for all  $H^* \geq 0$ ,  $Q(H^*) < 0$ . In this case, Model (3) has no interior equilibria.

(ii) Let  $r - B^* d_b > 0$ . By  $Q'(H^*) = -3d_h H^{*2} + 2(r - B^* d_b) H^* - d_h K$ , we have two cases:

(1) If  $\Delta = 4(r - B^* d_b)^2 - 12Kd_h^2 \leq 0$ , then for all  $H^* \in \mathbb{R}$ ,  $Q'(H^*) \leq 0$ . Notice  $Q(0) < 0$ , we know that for all  $H^* \geq 0$ ,  $Q(H^*) < 0$ . This implies that Model (3) has no interior equilibria for this case.

(2) If  $\Delta = 4(r - B^* d_b)^2 - 12Kd_h^2 > 0$ , i.e.,  $d_h < \frac{r - B^* d_b}{\sqrt{3K}}$ , then  $Q'(H^*)$  has two positive roots  $H_1^c < H_2^c$ :

$$H_{1,2}^c = \frac{(r - d_b B^*) \pm \sqrt{(r - d_b B^*)^2 - 3Kd_h^2}}{3d_h},$$

in which  $H_1^c$  is the minimum point and  $H_2^c$  is the maximum point of  $Q(H^*)$ .

- If  $Q(H_2^c) \leq 0$ , then for all  $H^* \geq 0$ ,  $Q(H^*) \leq 0$  and Model (3) has no interior equilibria.
- If  $Q(H_2^c) > 0$ , then  $Q(H^*)$  has exact two positive roots, denoted as  $H_1^r < H_2^r$ , satisfying  $Q(H^*) > 0$  for  $H^* \in (H_1^r, H_2^r)$  and  $Q(H^*) \leq 0$  for  $H^* \in [0, H_1^r] \cup [H_2^r, \infty)$ .

Thus, in order to show the existence of at least one interior equilibria, we only need to find a root of  $f_1(H^*) = f_2(H^*)$  in  $(H_1^r, H_2^r)$ .

Note that  $f_1(H^*)$  and  $f_2(H^*)$  have the following properties.

- $f_1(0) = 0$ ,  $\lim_{H \rightarrow \infty} f_1(H^*) = r$ , and  $f_1(H^*)$  is strictly increasing on  $[0, \infty)$ , which implies  $f_1(H_1^r) < f_2(H_2^r)$ .
- $\lim_{H^* \rightarrow 0} f_2(H^*) = \frac{B^*}{\tau} > 0$ ,  $\lim_{H^* \rightarrow \infty} f_2(H) = 0$  since  $\lim_{H^* \rightarrow \infty} M^*(H^*) = -\infty$ .
- $f_2(H_1^r) = f_2(H_2^r) = \frac{B^* d_b}{1 - e^{-\tau d_b}}$  since  $M(H_1^r) = M(H_2^r) = 0$ .
- By (20) and the fact  $M(H_1^r) = M(H_2^r) = 0$ ,  $f_2(H_1^r) = B^* d_b + d_h H_1^r$ ,  $f_2(H_2^r) = B^* d_b + d_h H_2^r$ , which implies  $f_2(H_1^r) > B^* d_b$ ,  $f_2(H_2^r) > B^* d_b$ .

From the properties (a) and (b), we can claim that if  $f_1(H_1^r) < f_2(H_1^r)$  and  $f_2(H_2^r) < f_1(H_2^r)$ , illustrated in Figure 11, then Model (3) has at least one interior equilibrium. Thus, by property (c), if  $\tau > 0$  satisfies the inequalities

$$f_1(H_1^r) < \frac{B^* d_b}{1 - e^{-\tau d_b}} < f_1(H_2^r), \quad (21)$$

then Model (3) has at least one interior equilibrium. Noticing property (d) and solving (21), we get

$$\beta_1 < \tau < \beta_2,$$

where

$$\beta_1 = \frac{1}{d_b} \ln \left( \frac{f_1(H_2^r)}{f_1(H_2^r) - B^* d_b} \right), \quad \beta_2 = \frac{1}{d_b} \ln \left( \frac{f_1(H_1^r)}{f_1(H_1^r) - B^* d_b} \right).$$

Therefore, if  $\tau \in (\beta_1, \beta_2)$ , then Model (3) has at least one interior equilibria.

At last, we give a sufficient condition, which is easy to be verified, such that  $Q(H_2^c) > 0$ . From the property of cubic function  $Q(H)$ , we know that it has unique point of inflection  $H_0 = \frac{r - B^* d_b}{3d_h}$ , and that if  $Q(H_0) > 0$  then  $Q(H_2^c) > 0$ . By a direct computation, we have

$$Q(H_0) = \frac{2(r - B^* d_b)^3}{27d_h^2} - \frac{K(r - B^* d_b)}{3} - d_b K B^*.$$

Thus, if

$$d_h < \frac{(r - B^* d_b) \sqrt{2(r - B^* d_b)}}{3\sqrt{K(r - B^* d_b) + 3d_b K B^*}}$$

then  $Q(H_0) > 0$ , and hence  $Q(H_2^c) > 0$ .



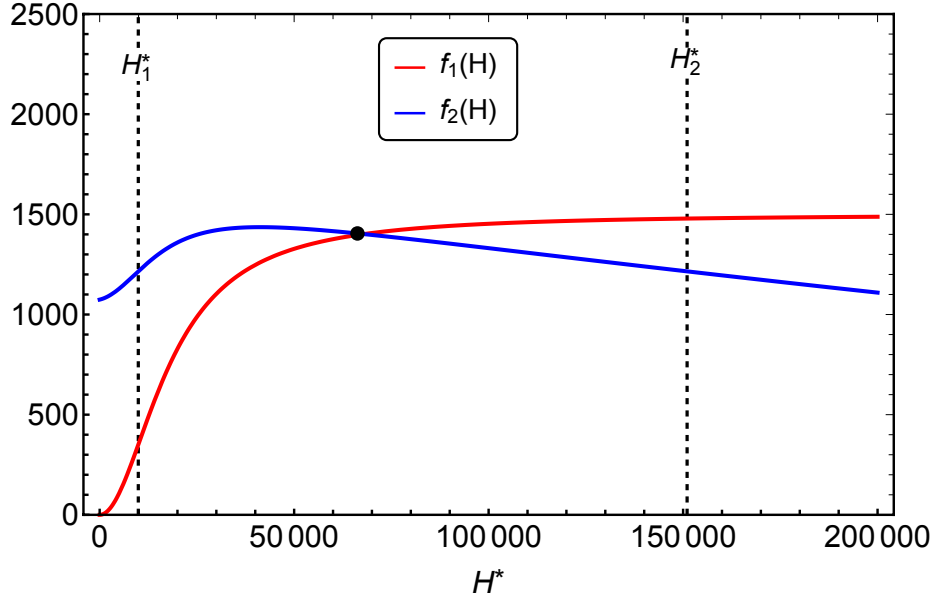


Figure 11: Graph showing the existence of a unique interior equilibrium whenever  $f_1(H^*) = f_2(H^*)$  occurring at the black dot with  $r = 1500$ ,  $K = 324000000$ ,  $d_b = 0.012$ ,  $d_h = 0.008$ ,  $d_m = 0.028$ ,  $\alpha_b = 0.038$ ,  $\alpha_h = 0.022$ ,  $c = 1.23$ ,  $a = 15100$ , and  $\tau = 21$ . Vertical dashed lines,  $H_1^*$  and  $H_2^*$ , are the positive solutions of  $Q(H^*)$  (eq. (11)).

□

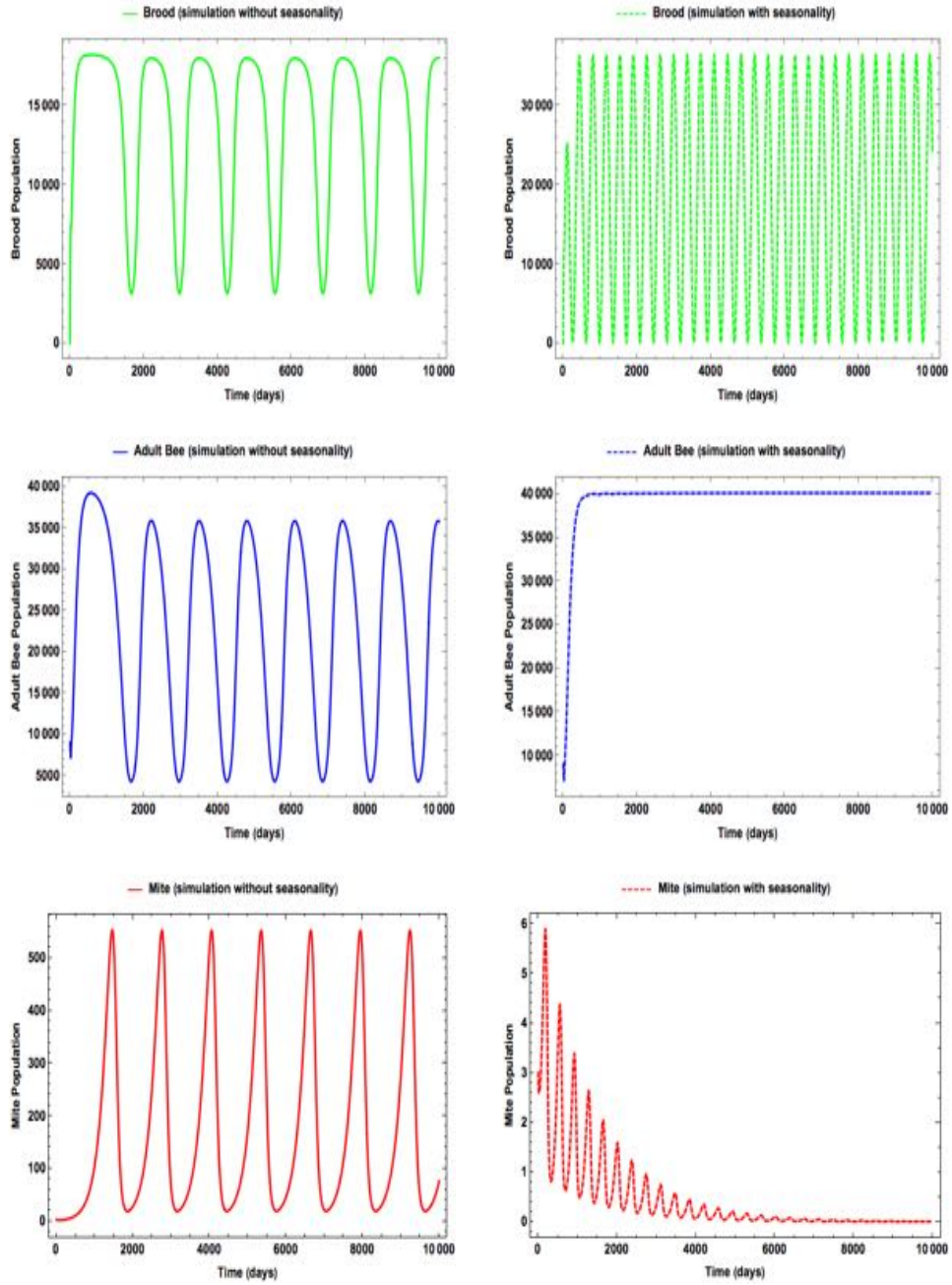
### Proof of Theorem 3.3

*Proof.* By the positivity of solutions of Model (2)-(3), the third equation of (3) implies that

$$\frac{dM}{dt} < (c\alpha_b - d_m)M(t) < 0,$$

since  $\frac{c\alpha_b}{d_m} < 1$ . Thus,  $\lim_{t \rightarrow \infty} M(t) = 0$ . Then, the model reduces to the model of Chen et al. [34], the global stability of  $E_{00}$ , we know that  $\lim_{t \rightarrow \infty} B(t) = \lim_{t \rightarrow \infty} H(t) = 0$  if  $d_h > \frac{re^{-d_b\tau}}{2\sqrt{K}}$ . The proof is complete. □

## Appendix B:



$$\alpha_b = 0.024$$

Figure 12: Time series of the brood, adult bee, and mites simulation using  $r = 1500$ ,  $K = 95000000$ ,  $d_b = 0.051$ ,  $d_h = 0.0121$ ,  $d_m = 0.027$ ,  $\alpha_h = 0.8$ ,  $c = 1.9$ ,  $a = 8050$ ,  $\tau = 21$ ,  $\Phi = 65$ ,  $B_0(t) = B(0) = 0$ ,  $H(0) = 9000$ , and  $M(0) = 3$  when the queen's eggs laying rate is constant in figures on the left column (i.e. no seasonality) and when the queen's eggs laying rate has seasonality in figures on the right column with  $\alpha_b = 0.024$ .

Parameters	PRCC		eFAST	
	sensitivity index	p-value	first-order $S_i$	total-order $S_{T_i}$
$r$	0.98441***	0	0.67936	0.68784
$\Phi$	0.48556***	2.7807e-60	0.0068948	0.0082977
$d_b$	-0.96544***	0	0.3079	0.31461
$d_h$	-0.51226***	5.3765e-68	0.0080172	0.0095901
$d_m$	0.012098	0.70239	3.7727e-05	0.00089457
$\alpha_b$	-0.055847	0.077527	0.00012458	0.0011038
$\alpha_h$	0.012944	0.68266	1.2504e-05	0.00081607
$a$	0.0469	0.13832	3.3803e-05	0.001148
$K$	-0.70529***	2.8295e-151	0.023235	0.024764
$c$	-0.074858*	0.017905	0.00014943	0.0010502
$\tau$	-0.36885***	1.3841e-33	0.0056511	0.006688

Table 3: Comparison of PRCC and eFAST Values at Time 96 and \* implies significance at 0.05 (i.e.  $p < 0.05$ ), \*\* is the significance at 0.01 (i.e.  $p < 0.01$ ), and \*\*\* implies significance at 0.001 (i.e.  $p < 0.001$ ).

## Acknowledgments

This research is partially supported by NSF-DMS (Award Number 1716802); NSF- IOS/DMS (Award Number 1558127) and The James S. McDonnell Foundation 21st Century Science Initiative in Studying Complex Systems Scholar Award (UHC Scholar Award 220020472). The research of K.M is also partially supported by the Department of Education GAANN (P200A120192). G.DH is partially supported by USDA-Areawide Research Grant.

## References

- [1] Aiello, W. G. and Freedman, H. (1990). A time-delay model of single-species growth with stage structure. *Mathematical biosciences*, 101(2):139–153.
- [2] Allen, M. and Ball, B. (1996). The incidence and world distribution of honey bee viruses. *Bee world*, 77(3):141–162.
- [3] Becher, M. A., Grimm, V., Thorbek, P., Horn, J., Kennedy, P. J., and Osborne, J. L. (2014). Beehave: a systems model of honeybee colony dynamics and foraging to explore multifactorial causes of colony failure. *Journal of Applied Ecology*, 51(2):470–482.
- [4] Betti, M. I., Wahl, L. M., and Zamir, M. (2014). Effects of infection on honey bee population dynamics: a model. *PloS one*, 9(10):e110237.

Parameters	PRCC		eFAST	
	sensitivity index	p-value	first-order $S_i$	total-order $S_{T_i}$
$r$	0.86644***	8.2575e-314	0.37861	0.4092
$\Phi$	0.067352*	0.033204	0.00082837	0.0034278
$d_b$	0.17398***	3.0723e-08	0.0046109	0.010879
$d_h$	-0.70591***	1.1773e-151	0.12011	0.1243
$d_m$	0.35619***	2.7923e-31	0.040672	0.10706
$\alpha_b$	-0.67827***	1.0389e-135	0.097734	0.1356
$\alpha_h$	-0.098217**	0.0018739	0.0040036	0.010628
$a$	0.28282***	7.56e-20	0.019395	0.043743
$K$	-0.35489***	4.7513e-31	0.020604	0.027903
$c$	-0.67647***	9.8499e-135	0.12116	0.21043
$\tau$	-0.5618***	2.9213e-84	0.01145	0.014629

Table 4: Comparison of PRCC and eFAST Values at Time 132 and \* implies significance at 0.05 (i.e.  $p < 0.05$ ), \*\* is the significance at 0.01 (i.e.  $p < 0.01$ ), and \*\*\* implies significance at 0.001 (i.e.  $p < 0.001$ ).

- [5] Boecking, O. and Spivak, M. (1999). Behavioral defenses of honey bees against varroa jacobsoni oud. *Apidologie*, 30(2-3):141–158.
- [6] Boot, W. J., Tan, N. Q., Dien, P. C., Van Huan, L., Van Dung, N., Beetsma, J., et al. (1997). Reproductive success of varroa jacobsoni in brood of its original host, apis cerana, in comparison to that of its new host, a. mellifera (hymenoptera: Apidae). *Bulletin of entomological research*, 87(02):119–126.
- [7] Branco, M. R., Kidd, N. A., and Pickard, R. S. (2006). A comparative evaluation of sampling methods for varroa destructor (acari: Varroidae) population estimation. *Apidologie*, 37(4):452.
- [8] Cacuci, D. G. and Ionescu-Bujor, M. (2004). A comparative review of sensitivity and uncertainty analysis of large-scale systems–ii: statistical methods. *Nuclear science and engineering*, 147(3):204–217.
- [9] Cervo, R., Bruschini, C., Cappa, F., Meconcelli, S., Pieraccini, G., Pradella, D., and Turillazzi, S. (2014). High varroa mite abundance influences chemical profiles of worker bees and mite–host preferences. *Journal of Experimental Biology*, 217(17):2998–3001.
- [10] De Jong, D., De Jong, P., and Goncalves, L. (1982). Weight loss and other damage to developing worker honeybees from infestation with varroa jacobsoni. *Journal of apicultural research*, 21(3):165–167.
- [11] DeGrandi-Hoffman, G., Ahumada, F., Curry, R., Probasco, G., and Schantz, L. (2014). Population growth of varroa destructor (acari: Varroidae) in commercial honey bee colonies treated with beta plant acids. *Experimental and Applied Acarology*, 64(2):171–186.

Parameters	PRCC		eFAST	
	sensitivity index	p-value	first-order $S_i$	total-order $S_{T_i}$
$r$	0.70392 ***	1.9182e-150	0.068869	0.11504
$\Phi$	0.2048 ***	6.248e-11	0.004525	0.013015
$d_b$	-0.59208 ***	1.2156e-95	0.030786	0.057749
$d_h$	-0.13905***	1.0195e-05	0.0021218	0.0058844
$d_m$	-0.77909 ***	1.3251e-204	0.05834	0.10418
$\alpha_b$	0.93967***	0	0.3487	0.010895
$\alpha_h$	-0.0751*	0.017538	0.0016142	0.041224
$a$	-0.5804 ***	4.1474e-91	0.016902	0.0093502
$K$	-0.27377***	1.1928e-18	0.0037531	0.41943
$c$	0.93868 ***	0	0.27371	Yes
$\tau$	-0.1642 ***	1.7756e-07	0.0012931	0.0043944

Table 5: Comparison of PRCC and eFAST Values at Time 183 and \* implies significance at 0.05 (i.e.  $p < 0.05$ ), \*\* is the significance at 0.01 (i.e.  $p < 0.01$ ), and \*\*\* implies significance at 0.001 (i.e.  $p < 0.001$ ).

- [12] DeGrandi-Hoffman, G., Ahumada, F., and Graham, H. (2017). Are dispersal mechanisms changing the host–parasite relationship and increasing the virulence of varroa destructor (mesostigmata: Varroidae) in managed honey bee (hymenoptera: Apidae) colonies? *Environmental entomology*, 46(4):737–746.
- [13] DeGrandi-Hoffman, G., Ahumada, F., Zazueta, V., Chambers, M., Hidalgo, G., and Watkins deJong, E. (2016). Population growth of varroa destructor (acari: Varroidae) in honey bee colonies is affected by the number of foragers with mites. *Experimental and Applied Acarology*, 69(1):21–34.
- [14] DeGrandi-Hoffman, G. and Curry, R. (2004). A mathematical model of varroa mite (varroa destructor anderson and truemana) and honeybee (apis mellifera l.) population dynamics. *International Journal of Acarology*, 30(3):259–274.
- [15] DeGrandi-Hoffman, G., Roth, S. A., Loper, G., and Erickson, E. H. (1989). Beepop: a honeybee population dynamics simulation model. *Ecological modelling*, 45(2):133–150.
- [16] DeGrandi-Hoffman, G., Wardell, G., Ahumada-Segura, F., Rinderer, T., Danka, R., and Pettis, J. (2008). Comparisons of pollen substitute diets for honey bees: consumption rates by colonies and effects on brood and adult populations. *Journal of apicultural research*, 47(4):265–270.
- [17] Del Piccolo, F., Nazzi, F., Della Vedova, G., and Milani, N. (2010). Selection of apis mellifera workers by the parasitic mite varroa destructor using host cuticular hydrocarbons. *Parasitology*, 137(6):967–973.

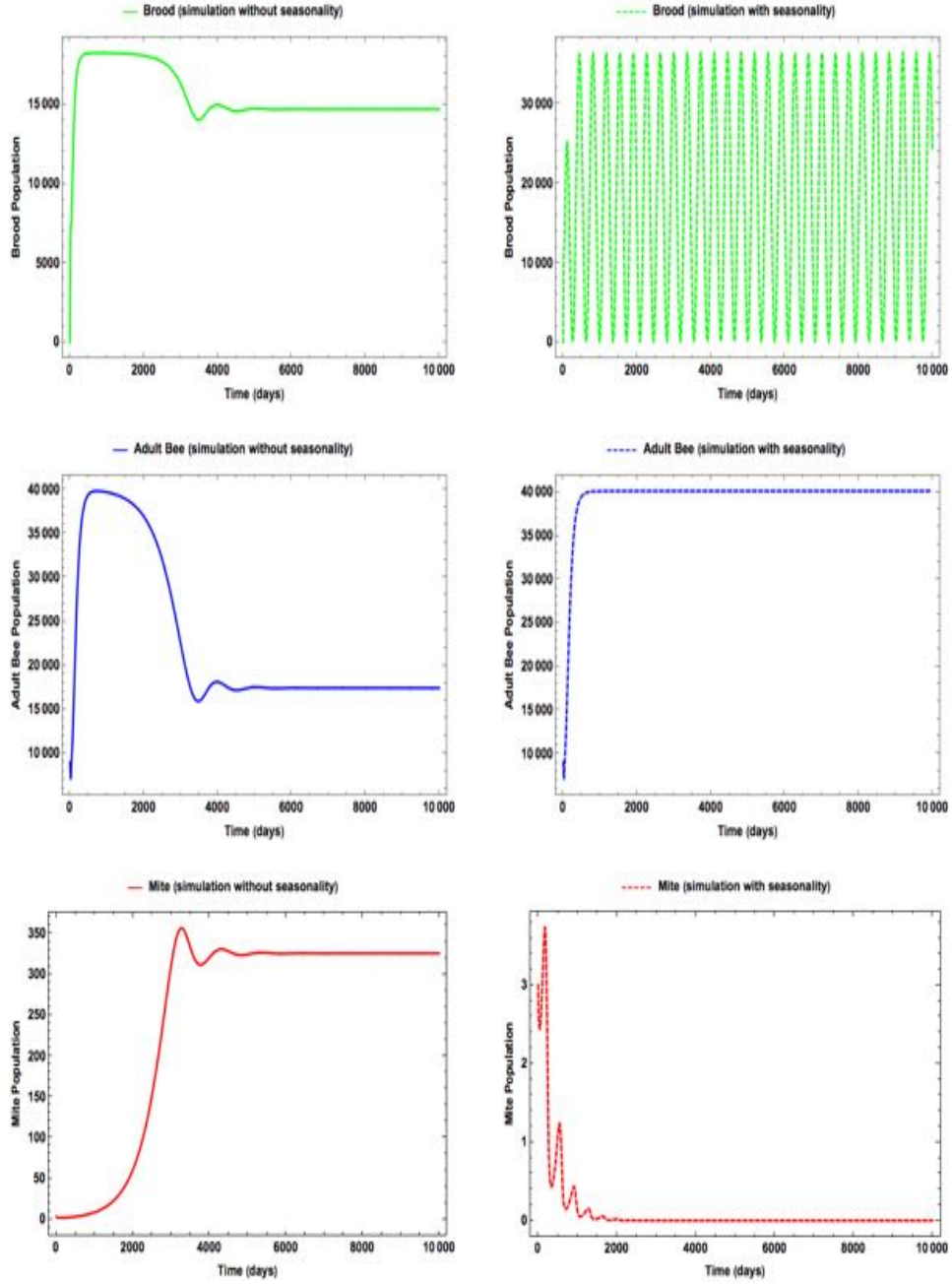
- [18] Donze, G., Herrmann, M., Bachofen, B., and GUERIN, P. R. M. (1996). Effect of mating frequency and brood cell infestation rate on the reproductive success of the honeybee parasite *varroa jacobsoni*. *Ecological entomology*, 21(1):17–26.
- [19] Doublet, V., Labarussias, M., de Miranda, J. R., Moritz, R. F., and Paxton, R. J. (2015). Bees under stress: sublethal doses of a neonicotinoid pesticide and pathogens interact to elevate honey bee mortality across the life cycle. *Environmental microbiology*, 17(4):969–983.
- [20] Eberl, H. J., Frederick, M. R., and Kevan, P. G. (2010). Importance of brood maintenance terms in simple models of the honeybee-varroa destructor-acute bee paralysis virus complex. *Electronic Journal of Differential Equations*, 19:85–98.
- [21] Eischen, F. A., Rothenbuhler, W. C., and Kulinčević, J. M. (1984). Some effects of nursing on nurse bees. *Journal of Apicultural Research*, 23(2):90–93.
- [22] Evans, J. D. and Spivak, M. (2010). Socialized medicine: individual and communal disease barriers in honey bees. *Journal of invertebrate pathology*, 103:S62–S72.
- [23] Feng, Z., Towers, S., and Yang, Y. (2011). Modeling the effects of vaccination and treatment on pandemic influenza. *The AAPS journal*, 13(3):427–437.
- [24] Fewell, J. H. and Winston, M. L. (1992). Colony state and regulation of pollen foraging in the honey bee, *apis mellifera* l. *Behavioral Ecology and Sociobiology*, 30(6):387–393.
- [25] Fukuda, H. and Sakagami, S. F. (1968). Worker brood survival in honeybees. *Researches on Population Ecology*, 10(1):31–39.
- [26] Garrido, C. and Rosenkranz, P. (2003). The reproductive program of female varroa destructor mites is triggered by its host, *apis mellifera*. *Experimental & applied acarology*, 31(3-4):269–273.
- [27] Genersch, E., Von Der Ohe, W., Kaatz, H., Schroeder, A., Otten, C., Büchler, R., Berg, S., Ritter, W., Mühlen, W., Gisder, S., et al. (2010). The german bee monitoring project: a long term study to understand periodically high winter losses of honey bee colonies. *Apidologie*, 41(3):332–352.
- [28] Graham, J. M. (1992). The hive and the honey bee. Technical report, Dadant & Sons Hamilton, IL.
- [29] Guzmán-Novoa, E., Eccles, L., Calvete, Y., McGowan, J., Kelly, P. G., and Correa-Benítez, A. (2010). Varroa destructor is the main culprit for the death and reduced populations of overwintered honey bee (*apis mellifera*) colonies in ontario, canada. *Apidologie*, 41(4):443–450.
- [30] Hayes Jr, J., Underwood, R. M., Pettis, J., et al. (2008). A survey of honey bee colony losses in the us, fall 2007 to spring 2008. *PloS one*, 3(12):e4071.
- [31] Huang, Z. (2012). Varroa mite reproductive biology. *American Bee Culture* <http://www.extension.org/pages/65450/varroa-mite-reproductivebiology>.
- [32] Iman, R. L. and Helton, J. C. (1988). An investigation of uncertainty and sensitivity analysis techniques for computer models. *Risk analysis*, 8(1):71–90.

- [33] Ionescu-Bujor, M. and Cacuci, D. G. (2004). A comparative review of sensitivity and uncertainty analysis of large-scale systems–i: Deterministic methods. *Nuclear science and engineering*, 147(3):189–203.
- [34] Jun Chen, Komi Messan, M. R. M. G. D.-H. D. B. and Kang, Y. (2020 submitted). How to model honeybee population dynamics: stage structure and seasonality. *Mathematics in Applied Sciences and Engineering*.
- [35] Kang, Y., Blanco, K., Davis, T., Wang, Y., and DeGrandi-Hoffman, G. (2016). Disease dynamics of honeybees with varroa destructor as parasite and virus vector. *Mathematical biosciences*, 275:71–92.
- [36] Klein, A.-M., Vaissiere, B. E., Cane, J. H., Steffan-Dewenter, I., Cunningham, S. A., Kremen, C., and Tscharntke, T. (2007). Importance of pollinators in changing landscapes for world crops. *Proceedings of the Royal Society of London B: Biological Sciences*, 274(1608):303–313.
- [37] Koleoglu, G., Goodwin, P. H., Reyes-Quintana, M., Hamiduzzaman, M. M., and Guzman-Novoa, E. (2017). Effect of varroa destructor, wounding and varroa homogenate on gene expression in brood and adult honey bees. *PloS one*, 12(1):e0169669.
- [38] Kralj, J., Brockmann, A., Fuchs, S., and Tautz, J. (2007). The parasitic mite varroa destructor affects non-associative learning in honey bee foragers, apis mellifera l. *Journal of Comparative Physiology A*, 193(3):363–370.
- [39] Kribs-Zaleta, C. M. and Mitchell, C. (2014). Modeling colony collapse disorder in honeybees as a contagion. *Mathematical biosciences and engineering: MBE*, 11(6):1275–1294.
- [40] Le Conte, Y., Ellis, M., and Ritter, W. (2010). Varroa mites and honey bee health: can varroa explain part of the colony losses? *Apidologie*, 41(3):353–363.
- [41] Linksvayer, T. A., Fondrk, M. K., and Page Jr, R. E. (2009). Honeybee social regulatory networks are shaped by colony-level selection. *The American Naturalist*, 173(3):E99–E107.
- [42] Marino, S., Hogue, I. B., Ray, C. J., and Kirschner, D. E. (2008). A methodology for performing global uncertainty and sensitivity analysis in systems biology. *Journal of theoretical biology*, 254(1):178–196.
- [43] Martin, S. (1998). A population model for the ectoparasitic mite varroa jacobsoni in honey bee (apis mellifera) colonies. *Ecological Modelling*, 109(3):267–281.
- [44] McKay, M. D., Beckman, R. J., and Conover, W. J. (1979). Comparison of three methods for selecting values of input variables in the analysis of output from a computer code. *Technometrics*, 21(2):239–245.
- [45] Messan, K., DeGrandi-Hoffman, G., Castillo-Chavez, C., and Kang, Y. (2017). e. *Mathematical Modelling of Natural Phenomena*, 12(2):84–115.
- [46] Navajas, M., Migeon, A., Alaux, C., Martin-Magniette, M.-L., Robinson, G., Evans, J., Cros-Arteil, S., Crauser, D., and Le Conte, Y. (2008). Differential gene expression of the honey bee apis mellifera associated with varroa destructor infection. *BMC genomics*, 9(1):301.

- [47] Neumann, P. and Carreck, N. L. (2010). Honey bee colony losses.
- [48] Oldroyd, B. P. (2007). What’s killing american honey bees? *PLoS biology*, 5(6):e168.
- [49] P. Magal, G.F. Webb, . Y. W. (2019). An environmental model of honey bee colony collapse due to pesticide contamination. *Journal of Mathematical Biology*, 81(X):4908–4931.
- [50] P. Magal, G.F. Webb, . Y. W. (2020). A spatial model of honey bee colony collapse due to pesticide contamination of foraging bees. *Journal of Mathematical Biology*, X(X):X.
- [51] Peck, D. T., Smith, M. L., and Seeley, T. D. (2016). Varroa destructor mites can nimbly climb from flowers onto foraging honey bees. *PloS one*, 11(12):e0167798.
- [52] Ratti, V., Kevan, P. G., and Eberl, H. J. (2012). A mathematical model for population dynamics in honeybee colonies infested with varroa destructor and the acute bee paralysis virus. *Canadian Applied Mathematics Quarterly: accepted*.
- [53] Ratti, V., Kevan, P. G., and Eberl, H. J. (2015). A mathematical model of the honeybee–varroa destructor–acute bee paralysis virus system with seasonal effects. *Bulletin of mathematical biology*, 77(8):1493–1520.
- [54] Rosenkranz, P., Aumeier, P., and Ziegelmann, B. (2010). Biology and control of varroa destructor. *Journal of invertebrate pathology*, 103:S96–S119.
- [55] Rueppell, O., Bachelier, C., Fondrk, M. K., and Page, R. E. (2007). Regulation of life history determines lifespan of worker honey bees (*apis mellifera* l.). *Experimental gerontology*, 42(10):1020–1032.
- [56] Saltelli, A. and Bolado, R. (1998). An alternative way to compute fourier amplitude sensitivity test (fast). *Computational Statistics & Data Analysis*, 26(4):445–460.
- [57] Schmickl, T. and Crailsheim, K. (2007). Hopomo: a model of honeybee intracolony population dynamics and resource management. *Ecological modelling*, 204(1):219–245.
- [58] Smith, H. L. (2011). *An introduction to delay differential equations with applications to the life sciences*, volume 57. Springer New York.
- [59] Steiner, J., Dittmann, F., Rosenkranz, P., and Engels, W. (1994). The first gonocycle of the parasitic mite (*varroa jacobsoni*) in relation to preimaginal development of its host, the honey bee (*apis mellifera carnica*). *Invertebrate reproduction & development*, 25(3):175–183.
- [60] Sumpter, D. J. and Martin, S. J. (2004). The dynamics of virus epidemics in varroa-infested honey bee colonies. *Journal of Animal Ecology*, 73(1):51–63.
- [61] van Dooremalen, C., Gerritsen, L., Cornelissen, B., van der Steen, J. J., van Langevelde, F., and Blacquière, T. (2012). Winter survival of individual honey bees and honey bee colonies depends on level of varroa destructor infestation. *PloS one*, 7(4):e36285.
- [62] Vanengelsdorp, D., Caron, D., Hayes, J., Underwood, R., Henson, M., Rennich, K., Spleen, A., Andree, M., Snyder, R., Lee, K., et al. (2012). A national survey of managed honey bee 2010–11 winter colony losses in the usa: results from the bee informed partnership. *Journal of Apicultural Research*, 51(1):115–124.



- [63] Wells, H. and Wells, P. H. (1986). Optimal diet, minimal uncertainty and individual constancy in the foraging of honey bees, *apis mellifera*. *The Journal of Animal Ecology*, pages 881–891.
- [64] Zimmerman, M. (1982). Optimal foraging: random movement by pollen collecting bumblebees. *Oecologia*, 53(3):394–398.



$$\alpha_b = 0.022$$

Figure 7: Time series of the brood, adult bee, and mites simulation using  $r = 1500$ ,  $K = 95000000$ ,  $d_b = 0.051$ ,  $d_h = 0.0121$ ,  $d_m = 0.027$ ,  $\alpha_h = 0.8$ ,  $c = 1.9$ ,  $a = 8050$ ,  $\tau = 21$ ,  $\Phi = 65$ ,  $B_0(t) = B(0) = 0$ ,  $H(0) = 9000$ , and  $M(0) = 3$  when the queen's eggs laying rate is constant in figures on the left column (i.e. no seasonality) and when the queen's eggs laying rate has seasonality in figures on the right column with  $\alpha_b = 0.022$ .

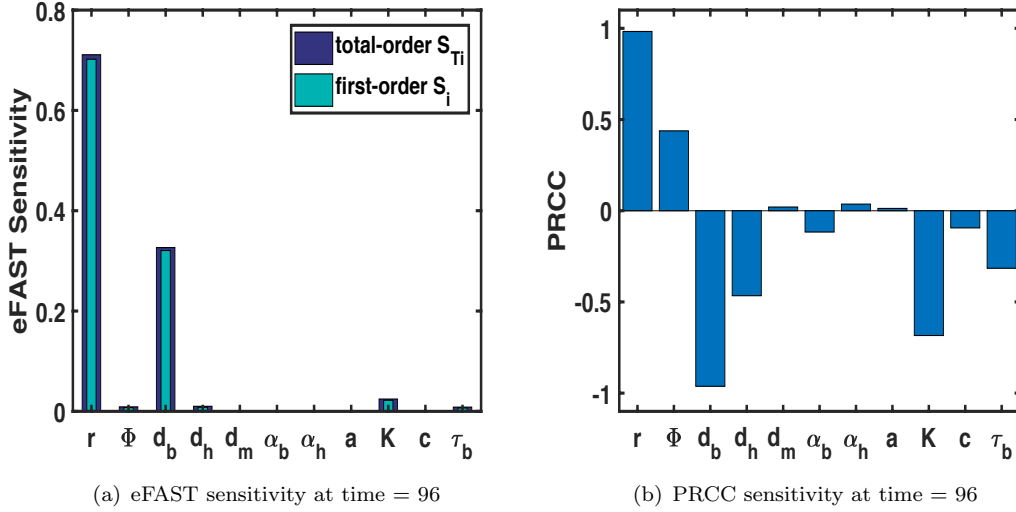


Figure 8: eFAST and PRCC Sensitivity analysis on Model (2) and (3) using parameter from Figures 6 where time point chosen correspond to the highest population point from the brood population in Figure 6(a). Figures 8(a) shows the eFAST results with resampling and search curves were resampled five times ( $N_R = 5$ ), for a total of 3575 model evaluations ( $N_S = 65$ ). First-order  $S_i$  and total-order  $S_{T_i}$  are shown for each parameter as shown in the legend. Figures 8(b) illustrates the result of the PRCC results with  $N = 1000$ .

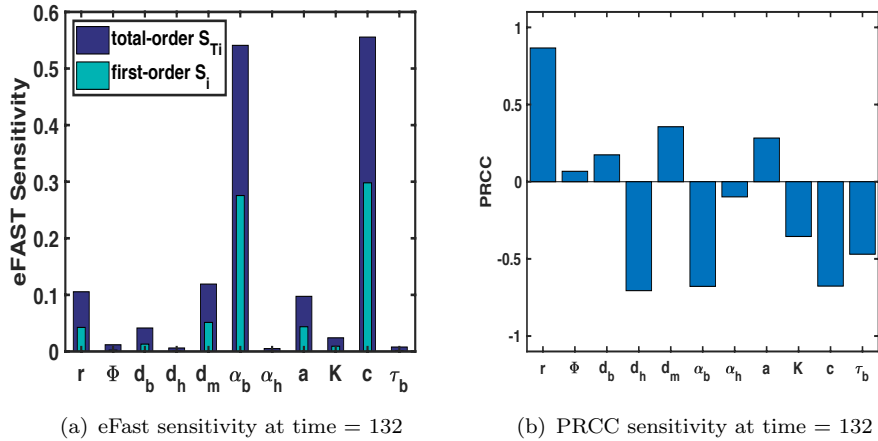
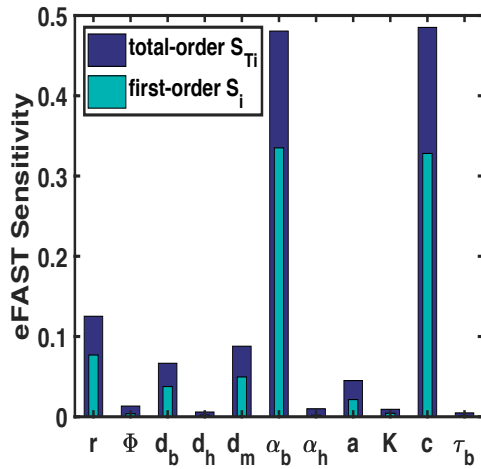
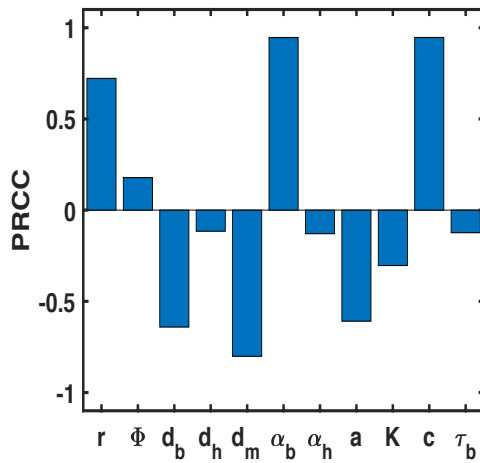


Figure 9: eFAST and PRCC Sensitivity analysis on Model (2) and (3) using parameter from Figures 6 where time point chosen correspond to the highest population point from the adult bee population in Figure 6(b). Figures 9(a) shows the eFAST results with resampling and search curves were resampled five times ( $N_R = 5$ ), for a total of 3575 model evaluations ( $N_S = 65$ ). First-order  $S_i$  and total-order  $S_{T_i}$  are shown for each parameter as shown in the legend. Figures 9(b) illustrates the result of the PRCC results with  $N = 1000$ .

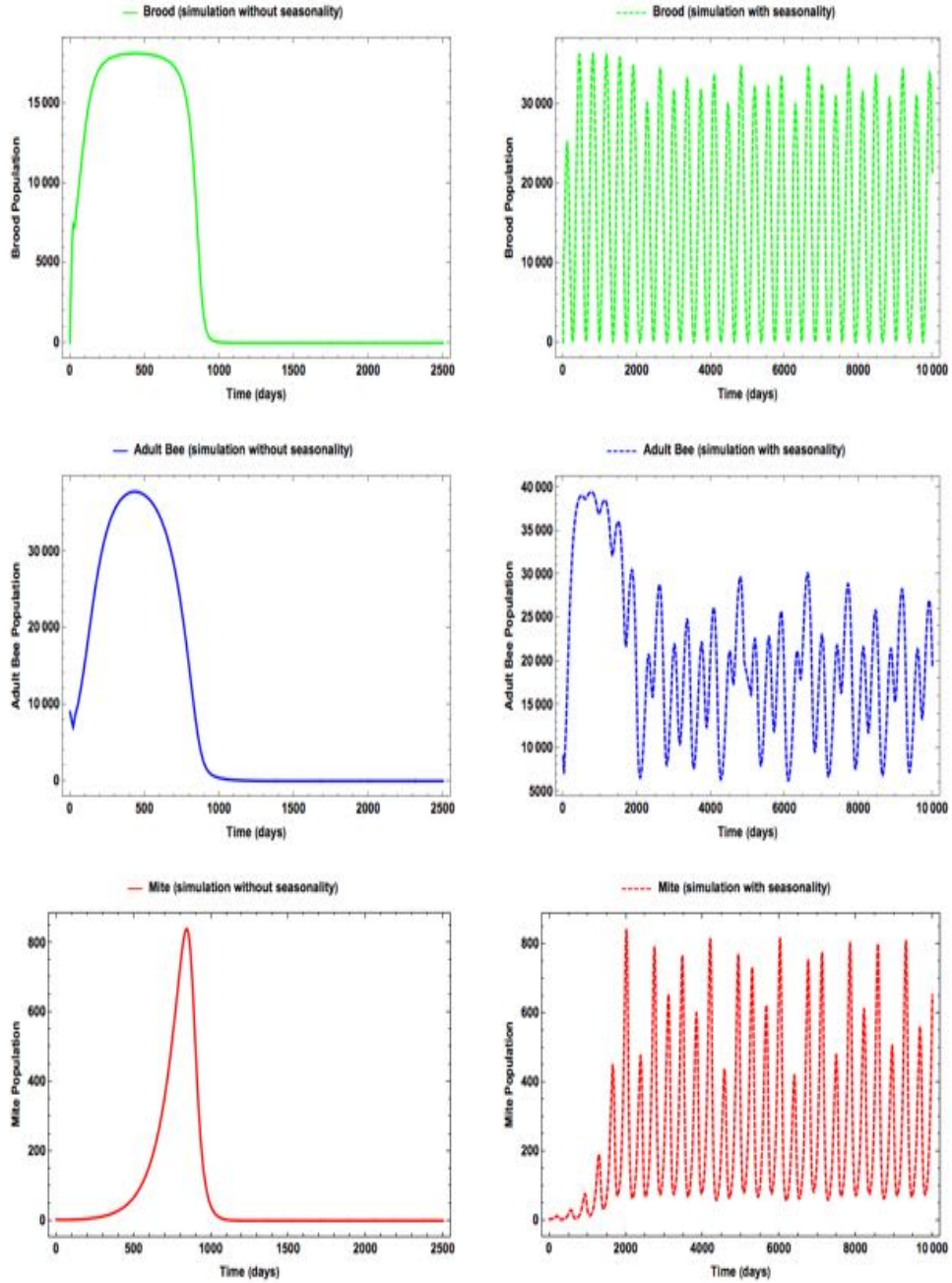


(a) eFast sensitivity at time = 183



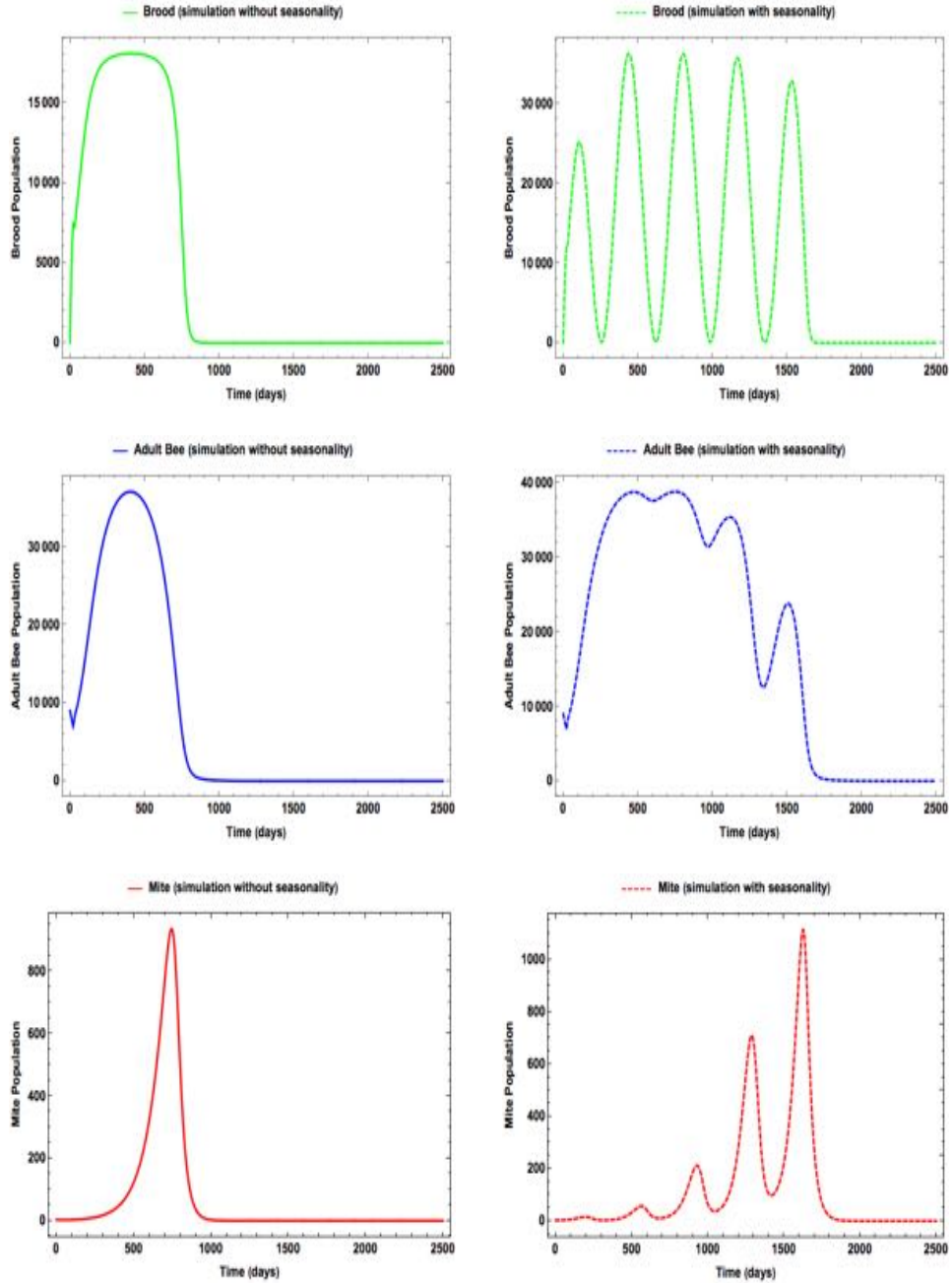
(b) PRCC sensitivity at time = 183

Figure 10: eFAST and PRCC Sensitivity analysis on Model (2) and (3) using parameter from Figures 6 where time point chosen correspond to the highest population point from the mite population in Figure 6(c). Figures 10(a) shows the eFAST results with resampling and search curves were resampled five times ( $N_R = 5$ ), for a total of 3575 model evaluations ( $N_S = 65$ ). First-order  $S_i$  and total-order  $S_{T_i}$  are shown for each parameter as shown in the legend. Figures 10(b) illustrates the result of the PRCC results with  $N = 1000$ .



$$\alpha_b = 0.027$$

Figure 13: Time series of the brood, adult bee, and mites simulation using  $r = 1500$ ,  $K = 95000000$ ,  $d_b = 0.051$ ,  $d_h = 0.0121$ ,  $d_m = 0.027$ ,  $\alpha_h = 0.8$ ,  $c = 1.9$ ,  $a = 8050$ ,  $\tau = 21$ ,  $\Phi = 65$ ,  $B_0(t) = B(0) = 0$ ,  $H(0) = 9000$ , and  $M(0) = 3$  when the queen's eggs laying rate is constant in figures on the left column (i.e. no seasonality) and when the queen's eggs laying rate has seasonality in figures on the right column with  $\alpha_b = 0.027$ .



$$\alpha_b = 0.028$$

Figure 14: Time series of the brood, adult bee, and mites simulation using  $r = 1500$ ,  $K = 95000000$ ,  $d_b = 0.051$ ,  $d_h = 0.0121$ ,  $d_m = 0.027$ ,  $\alpha_h = 0.8$ ,  $c = 1.9$ ,  $a = 8050$ ,  $\tau = 21$ ,  $\Phi = 65$ ,  $B_0(t) = B(0) = 0$ ,  $H(0) = 9000$ , and  $M(0) = 3$  when the queen's eggs laying rate is constant in figures on the left column (i.e. no seasonality) and when the queen's eggs laying rate has seasonality in figures on the right column with  $\alpha_b = 0.028$ .